D'Arcy, M., Schildgen, T., Strecker, M. R., Wittmann, H., Duesing, W., Mey, J., Tofelde, S., Weissmann, P., Alonso, R. N. (2019): Timing of past glaciation at the Sierra de Aconquija, northwestern Argentina, and throughout the Central Andes. - *Quaternary Science Reviews*, *204*, pp. 37—57.

DOI: http://doi.org/10.1016/j.quascirev.2018.11.022

# Timing of past glaciation at the Sierra de Aconquija, northwestern Argentina, and throughout the Central Andes

Mitch D'Arcy[1,2]*; Taylor F. Schildgen[2,1]; Manfred R. Strecker[1]; Hella Wittmann[2]; Walter Duesing[1]; Jürgen Mey[2]; Stefanie Tofelde[1,2]; Philipp Weissmann[1]; Ricardo N. Alonso[3]

[1]Institute of Earth and Environmental Science, University of Potsdam, Karl-Liebknecht-Strasse 24/25, 14476 Potsdam, Germany

[2]GFZ German Research Centre for Geosciences, Telegrafenberg, 14473 Potsdam, Germany

[3]Departamento de Geología, Universidad Nacional de Salta and CONICET (CEGA-INSUGEO), 4400 Salta, Argentina

*Corresponding author. Email: mdarcy@uni-potsdam.de; Phone: +49 331 2882 8832.

Published in *Quaternary Science Reviews*, **204**, 37-57.

Full citation:

D'Arcy, M., Schildgen, T.F., Strecker, M.R., Wittmann, H., Duesing, W., Mey, J., Tofelde, S., Weissmann, P., Alonso, R.N. (2019) Timing of past glaciation at the Sierra de Aconquija, northwestern Argentina, and throughout the Central Andes. *Quaternary Science Reviews*, **204**, 37-57.

## Abstract

Advances in cosmogenic nuclide exposure dating have made moraines valuable terrestrial recorders of palaeoclimate. A growing number of moraine chronologies reported from the Central Andes show that tropical glaciers responded sensitively to past changes in precipitation and temperature over timescales ranging from $10^3$ to $10^5$ years. However, the causes of past glaciation in the Central Andes remain uncertain. Explanations have invoked insolation-modulated variability in the strength of the South American Summer Monsoon, teleconnections with the North Atlantic Ocean, and/or cooling in the Southern Hemisphere. The driver for these past climate changes is difficult to identify, partly due to a lack of dated moraine records, especially in climatically sensitive areas of the southern Central Andes. Moreover, new constraints are needed on precisely where and when glaciers advanced. We use cosmogenic $^{10}$Be produced in situ to determine exposure ages for three generations of moraines at the Sierra de Aconquija, situated at 27°S on the eastern flank of the southern Central Andes. These moraines record glacier advances at approximately 22 ka and 40 ka, coincident with summer insolation maxima in the sub-tropics of the Southern Hemisphere, as well as at 12.5 ka and 13.5 ka during the Younger Dryas and the Antarctic Cold Reversal, respectively. We also identify minor glaciation during Bond Event 5, also known as the 8.2 ka event. These moraines register past climate changes with high fidelity, and currently constitute the southernmost dated record of glaciation on the eastern flank of the Central Andes. To contextualise these results, we compile $^{10}$Be data reported from 144 moraines in the eastern Central Andes that represent past glacier advances. We re-calculate exposure ages from these data using an updated reference production rate, and we re-interpret the moraine ages by taking the oldest clustered boulder age (after the exclusion of outliers attributed to nuclide inheritance) as closest to the timing of glacier advance—an approach for which we provide empirical justification. This compilation reveals that Central Andean glaciers have responded to changes in temperature and precipitation. We identify cross-latitude advances in phase with insolation cycles, the last global glacial maximum, and episodes of strengthened monsoonal moisture transport including the Younger Dryas and Heinrich Stadials 1 and 2. Our results from the Sierra de Aconquija allow us to constrain the southerly limit of enhanced precipitation associated with Heinrich Stadials at ~25°S. More broadly, our findings demonstrate at both local and regional scales that moraines record past climate variability with a fine spatial and temporal resolution.

Keywords:

Glaciation; Palaeoclimatology; South America; Cosmogenic isotopes; Monsoon; Younger Dryas; Antarctic Cold Reversal; Central Andes; Moraines

## 1. Introduction

Much of the Central Andes are currently unglaciated due to the relatively warm and dry climate in this region. However, during the past several tens of thousands of years, the Central Andes experienced glacial advances during cooler and wetter episodes associated with orbital cycles and millennial-scale climate events (Smith et al., 2005a,b; Jomelli et al., 2014; Bromley et al., 2016; Martini et al., 2017; Ward et al., 2017). These climate changes have been reconstructed using archives and proxies including lake cores and shorelines (Sylvestre et al., 1999; Baker et al., 2001; Placzek et al., 2006, 2013; Baker and Fritz, 2015), plant fossils and pollen (Chepstow-Lusty et al., 2005; Maldonado et al., 2005; Torres et al., 2016), stable isotopes (Cruz et al., 2005; Wang et al., 2007; Kanner et al., 2012), ice cores (Thompson et al., 1995, 1998; Ramirez et al., 2003), biomarkers (Fornace et al., 2016), and basin sediments (Nester et al., 2007; Steffen et al., 2009, 2010; Bekaddour et al., 2014; Schildgen et al., 2016; Tofelde et al., 2017). Moraines also provide valuable site-specific records of cooler and wetter conditions, and can be dated to constrain the timings of past glacial advances (Tapia, 1925; Rohmeder, 1941).

A growing number of records collectively show that palaeoclimate changes in the Central Andes have been partly governed by insolation-driven cycles of strengthening and weakening of the South American Summer Monsoon (SASM) (Baker and Fritz, 2015, provides a review). The SASM transfers tropical Atlantic moisture across the Amazon basin and southward along the eastern side of the Central Andes during the austral summer (Garreaud et al., 2003; Vera et al., 2006; Marengo et al., 2012), and its intensity is correlated with warm temperatures and a southerly position of the Inter-Tropical Convergence Zone (ITCZ) in the western tropical Atlantic Ocean (Zhang et al., 2016; Portilho-Ramos et al., 2017; Novello et al., 2017; Crivellari et al., 2018). During insolation maxima in the southern tropics—most recently at ~20 ka and ~40 ka—the SASM was strengthened, and the climate of the Central Andes was wetter, with deeper and fresher lakes (Baker et al., 2001), more depleted $\delta^{18}O$ archives (Thompson et al., 1998; Ramirez et al., 2003), and advancing glaciers (Martini et al., 2017; Ward et al., 2015). At insolation minima, such as during the early- to mid-Holocene, the Central Andes experienced a drier climate as the SASM weakened (Baker and Fritz, 2015). In addition to insolation cycles, the strength of the SASM has been modulated by millennial-scale events in the Atlantic Ocean, including Heinrich Stadials and the Younger Dryas (Zhang et al., 2015;

Portilho-Ramos et al., 2017). As a result, glaciers throughout the Central Andes have responded to climate fluctuations acting over a range of superposing timescales, and dated moraines offer an opportunity to reconstruct past climate variability. However, despite a growing number of dated moraine records, uncertainties persist regarding (i) the precise timings and spatial variability of advances throughout the Central Andes (Smith et al., 2005a,b; Bromley et al., 2009; Shakun et al., 2015); (ii) whether advances and retreats were primarily driven by changes in temperature, precipitation, or a combination of both (Jomelli et al., 2014; Ward et al., 2015; Bromley et al., 2016); and (iii) the responses of glaciers at different latitudes to short-lived (~1 kyr) climate events, including Heinrich Stadials (HS), the Antarctic Cold Reversal (ACR), and the Younger Dryas (YD) (Blard et al., 2009; Jomelli et al., 2014). New dated moraines would help address some of these knowledge gaps, especially in the semi-arid southern part of the Central Andes where moraine records are sparse but sensitivity to climate changes is high (Rodbell et al., 2009; Sagredo et al., 2014; Terrizzano et al., 2017).

Here, we use the terrestrial cosmogenic nuclide $^{10}$Be to determine new exposure ages for three generations of moraines at the Sierra de Aconquija, located at 27°S in northwestern Argentina. These moraines now constitute the southern-most dated record of past glaciation along the eastern flank of the southern Central Andes. We compare this new chronology with an updated compilation of moraine ages from other parts of the Central Andes. In this compilation, we (i) recalculate exposure ages from previously reported $^{10}$Be cosmogenic nuclide data with a new production rate calibration; (ii) standardise the interpretation of boulder-age clusters across all study locations; and (iii) distinguish between more and less reliable data. The age compilation reveals subtle latitudinal variations in the timings of glacier advances during the past ~45 ka. Additionally, the compilation shows that glaciers advanced in the Central Andes in response to short-lived strengthening of the SASM during the Younger Dryas and Heinrich Stadials 1 and 2. During Heinrich Stadials in particular, our results from the Sierra de Aconquija help to constrain a southerly limit of enhanced precipitation at ~25°S.

# 2. Study Area

## 2.1. The Sierra de Aconquija

The Sierra de Aconquija is located at 27°S and 66°W, on the eastern flank of the southern Central Andes (Fig. 1). The range has peak elevations exceeding 5000 m and forms a major topographic barrier to moisture transported from the northeast. Currently, there are no glaciers on the Sierra de Aconquija, although small and stationary rock glaciers are present above 4800 m in restricted, shaded locations (Haselton et al., 2002; Ahumada et al., 2013; Fig. 2). The Sierra de Aconquija has experienced multiple glaciations in the past, as documented by

moraines and cirques on both sides of the range (Tapia, 1925; Rohmeder, 1941). Moraine elevations average 400 m higher on the western side, reflecting the easterly moisture source and a strong orographic precipitation gradient across the range (Haselton et al., 2002; see Section 2.2).

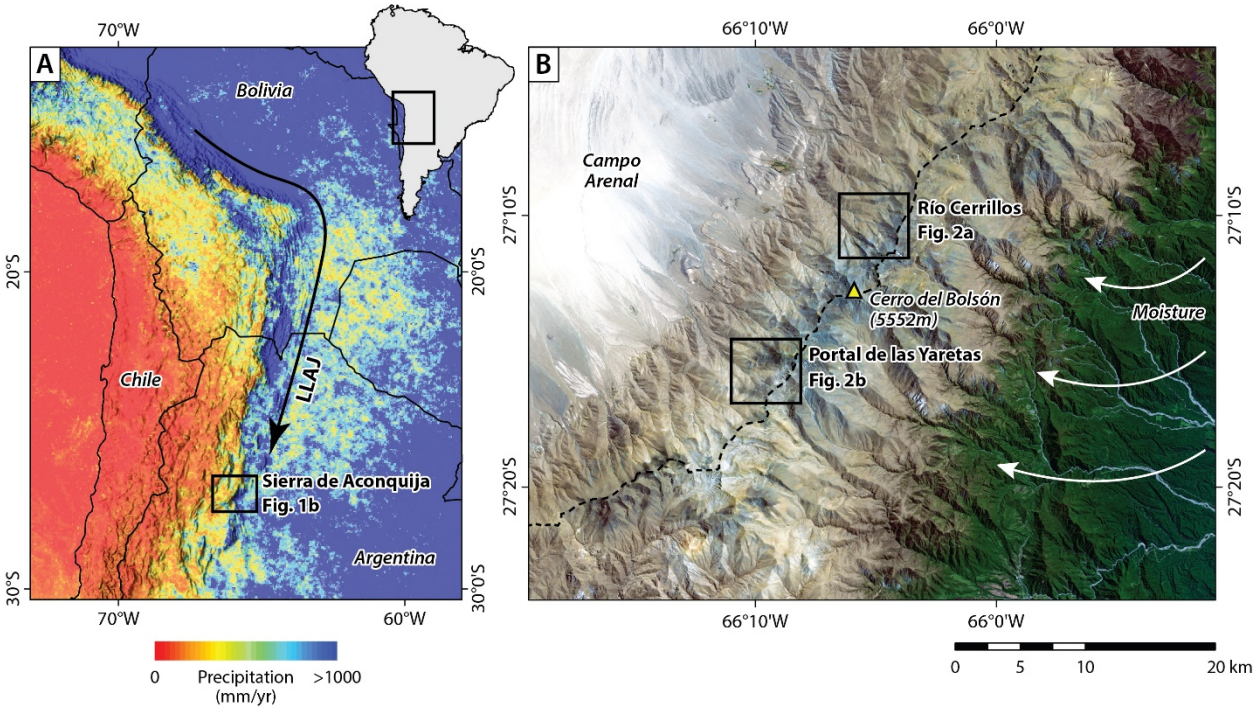


**Fig. 1. (A)** Location of the Sierra de Aconquija in the southern Central Andes. The colours indicate annual rainfall rates from TRMM 2B31 (Bookhagen and Strecker, 2008). Rainfall associated with the Low Level Andean Jet (LLAJ) is pronounced along the eastern flank of the Andes. **(B)** Landsat-8 true colour composite of the Sierra de Aconquija indicating the two sampled glacial valleys on the western side of the drainage divide (dashed line). Due to the highly asymmetric distribution and amount of rainfall across the Sierra de Aconquija the vegetation cover is denser on the eastern windward side of the range.

For our moraine boulder sampling, we targeted two different valleys on the western side of the Sierra de Aconquija that contain three generations of well-preserved lateral and end moraines situated at an elevation of 4000-4800 m. These are the Río Cerrillos valley and the Portal de las Yaretas valley (Fig. 1b, Fig. 2), situated north and south of the Cerro del Bolsón peak (5552 m; 27.213°S, 66.094°W), respectively. Both catchments erode a combination of gneiss and granite bedrock (Strecker et al., 1989).

The three different moraine generations, which we denote as M1, M2, and M3, are distinguished on the basis of cross-cutting relationships and their morphological properties. The oldest moraine unit, M1, represents the largest advance in the Río Cerrillos catchment

because the lateral moraines occupy the widest parts of the valleys. These features have crests 30-40 m higher than adjacent moraines and relatively smooth topographic relief with fewer protruding surface boulders. The younger M2 lateral moraines exhibit more depositional texture and are inset into the M1 moraines, meaning they must be younger. The youngest M3 moraines cross-cut both M1 and M2 in the Río Cerrillos catchment. They also represent the smallest advance, with narrowly spaced lateral moraines and well-preserved textural relief and rougher surfaces with more protruding boulders. End moraines can be clearly identified within the M3 units (marked with black lines in Fig. 2). The Portal de las Yaretas is a narrower valley, which was completely resurfaced by the youngest M3 advance. Several end moraines are preserved here; these could be recessional moraines, representing hiatuses during the retreat of a more extensive glacier, or they could be terminal moraines formed as the glacier repeatedly retreated and re-advanced; we revisit this question later. Large boulders (>1 m diameter) suitable for dating are present on all moraine surfaces (see Section 3).

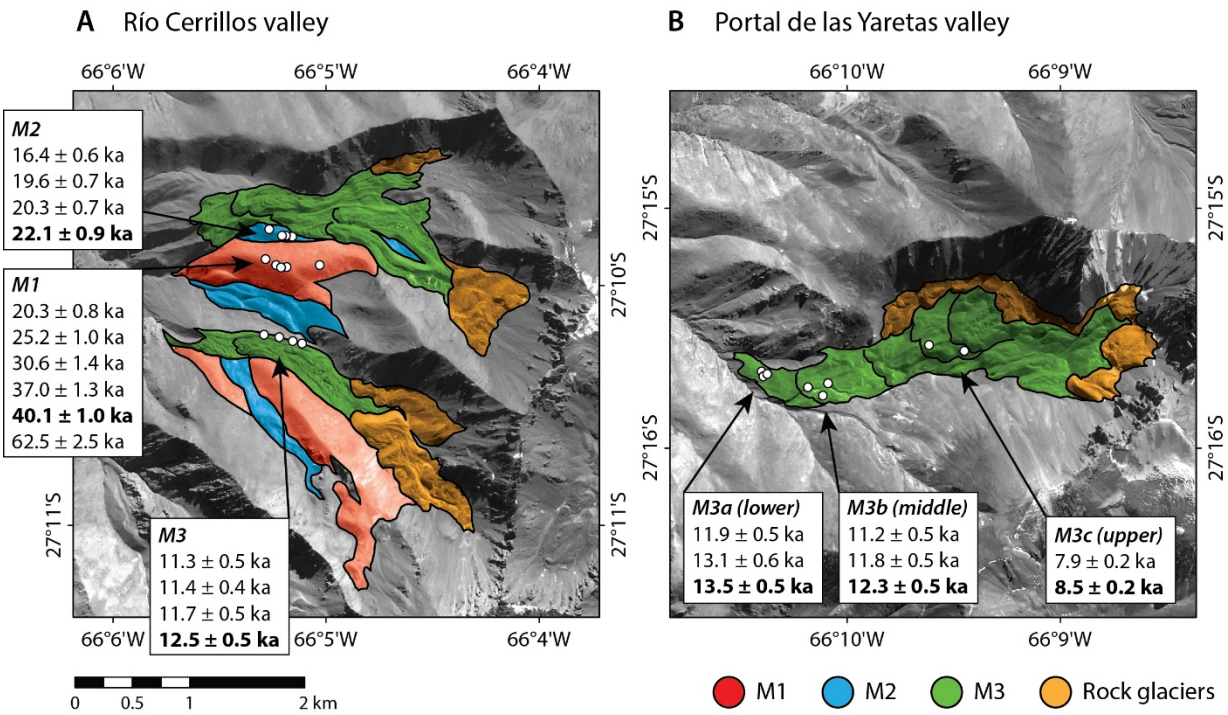


**Fig. 2.** Detailed maps of the moraines dated in this study. **(A)** Río Cerrillos valley. **(B)** Portal de las Yaretas valley. Boulder locations are marked with white dots, and ages are indicated for each location with the oldest age in each cluster highlighted in bold (see text for details).

## 2.2. Modern and past climate

The Sierra de Aconquija is located at the southern limit of the dry Central Andes (15 to 27°S), directly east of the arid/semi-arid Puna Plateau and the hyper-arid Atacama Desert (Bianchi and Yañez, 1992; Strecker et al., 2007). Rainfall is highly seasonal, with approximately 80% of annual precipitation arriving between November and February from Atlantic sources, via the Amazon, during the South American Summer Monsoon (SASM) (Prohaska, 1976; Zhou and Lau, 1998; Garreaud et al., 2003; Bookhagen and Strecker, 2008; Marengo et al., 2012; Castino et al., 2016). Much of this monsoonal moisture is transported southwards along the eastern flank of the Central Andes by the Low Level Andean Jet (LLAJ; Vera et al., 2006) (Fig. 1a). The Sierra de Aconquija is located at what is approximately the current southern limit of the LLAJ. As such, the range experiences a strong east-west orographic gradient in annual precipitation rates, which decline from >2000 mm $yr^{-1}$ in the densely vegetated eastern foothills to ~300 mm $yr^{-1}$ in the catchment headwaters at 4000-5000 m elevation, and further to ~250 mm $yr^{-1}$ in the semi-arid Campo Arenal basin to the west (Fig. 1b). For a more detailed review of the present climate of the Southern Central Andes, we refer to Strecker et al. (2007).

In the past, the climate in South America has fluctuated over various timescales, shifting between wetter and drier conditions. For a review, see Baker and Fritz (2015). Over the timescales considered in this study, important climate changes have occurred in association with (i) orbitally-driven insolation cycles in the Southern Hemisphere and (ii) millennial-scale climate events during the last glacial termination.

As insolation has oscillated in the tropics in phase with 19-25 kyr precessional cycles, the position of the Inter-Tropical Convergence Zone (ITCZ) in the Atlantic Ocean has been displaced, leading to changes in the overall intensity of the SASM and thereby in moisture transport to the Central Andes (Garreaud et al., 2003; Cook and Vizy, 2006; Baker and Fritz, 2015). Palaeoclimate records show that wetter conditions prevailed at insolation maxima, and drier conditions prevailed at insolation minima. The two most recent sustained wet periods in the Central Andes caused by intensification of the SASM at insolation maxima were the 'Tauca' interval (15-26 ka) and the 'Minchin' interval (36-48 ka), as defined by dating of lacustrine cores on the Bolivian Altiplano (Baker et al., 2001a,b). During these pluvial phases, lakes were deeper and fresher (Baker et al., 2001a,b; Bobst et al., 2001; Bookhagen et al., 2001; Placzek et al., 2006, 2013; Fritz et al., 2007; Hillyer et al., 2009; Blard et al., 2011), mountain glaciers advanced (Clapperton et al., 1997; Smith et al., 2005a,b; Zech et al., 2008, 2009b; Blard et al., 2009; Hall et al., 2009; Ward et al., 2015; Martini et al., 2017; Martin et al., 2018), negative excursions occurred in terrestrial $\delta^{18}O$ records (Cruz et al., 2005; Wang et al., 2007; Cheng et al., 2013), and landscapes responded to increased rainfall rates with enhanced landsliding and adjustments to fluvial aggradation-incision patterns (Trauth et al., 2000, 2003; Tchilinguirian

and Pereyra, 2001; Steffen et al., 2009, 2010; Schildgen et al., 2016; Tofelde et al., 2017). It should be noted that some studies use the term 'Tauca' to refer to a shorter-lived wet episode at 18.0-14.7 ka, which coincides with Heinrich Stadial 1 (e.g., Blard et al., 2011, 2013), and there is debate about the attribution of particular lake shorelines to the 'Minchin' period (Placzek et al., 2006; Baker and Fritz, 2015). In this paper, we use the terms 'Tauca' and 'Minchin' to refer to the pluvial episodes associated with insolation maxima.

On shorter (millennial) timescales, abrupt cold events in the North Atlantic Ocean also modulated the position of the ITCZ and the resulting intensity of the SASM (Peterson et al., 2000; Baker et al., 2001a; Haug et al., 2001; Chiang et al., 2003; Montade et al., 2015). These include Heinrich events, the Younger Dryas (YD; 12.9-11.7 ka), and Bond events (Baker and Fritz, 2015). For example, during Heinrich Stadial 1 (HS1; 18.0-14.7 ka) the ITCZ in the tropical Atlantic was displaced 5° southward of its modern position, linked to a slowdown of the Atlantic Meridional Overturning Circulation (AMOC) and a decline in heat transport across the Equator (Portilho-Ramos et al., 2017). Sea surface temperatures off the northeastern coast of Brazil increased by 2-3 °C, rising from 17.8 ka and peaking at ~15 ka (Crivellari et al., 2018). This warming resulted in a transient intensification of the SASM and greater precipitation rates in the Central Andes, as recorded by speleothems (Kanner et al., 2012; Mosblech et al., 2012; Cheng et al., 2013; Novello et al., 2017), ice cores (Thompson et al., 1995), palaeo-lake shorelines (Placzek et al., 2006, 2013; Blard et al., 2011), palaeo-lake cores (Baker et al., 2001), and sediment loads exported to the Amazon basin (Crivellari et al., 2018). Similarly, the YD is recorded as a significant negative excursion in terrestrial $\delta^{18}O$ records from both speleothems in Peru (Cheng et al., 2013) and southeast Brazil (Cruz et al., 2005; Wang et al., 2007), as well as in ice cores in Peru and Bolivia (Thompson et al., 1995; Ramirez et al., 2003) and high Altiplano lake levels (Blard et al., 2011). Collectively, these palaeoclimate records indicate wetter conditions in the Central Andes during Heinrich Stadials and the YD, associated with cold events in the North Atlantic, southward displacement of the ITCZ and strengthening of the SASM (Mosblech et al., 2012; Novello et al., 2017; Zhang et al., 2017; Crivellari et al., 2018).

However, there is still a lack of consensus as to whether Central Andean glaciers responded uniformly to these short-lived episodes of intensified monsoonal moisture transport. Some studies have associated dated moraines with the YD (Glasser et al., 2009; Rodbell et al., 2009; Zech et al., 2010; Kelly et al., 2012; Martini et al., 2017), but this correlation can be difficult to demonstrate unambiguously when calculated ages have uncertainties of ~1 ka and the YD interval only lasted from 12.9 ka to 11.7 ka (Bromley et al., 2011; Ward et al., 2015). Jomelli et al. (2014) suggested that moraine ages may instead correlate with the slightly earlier Antarctic Cold Reversal (ACR; 14.7-13.0 ka), as supported by high-precision dating of a moraine system

in Colombia (Jomelli et al., 2014), a compilation of revised ages across the Central Andes (Jomelli et al., 2017), and some additional moraine chronologies from individual locations (e.g., Stansell et al., 2017). The ACR was an abrupt cooling event in the Southern Hemisphere that pre-dated the YD, coinciding with the Bølling-Allerød interstadial in the Northern Hemisphere (Blunier et al., 1997). South of 40°S the ACR is the dominant climate event recorded by palaeoclimate archives since the LGM (Pedro et al., 2016); for example it caused glaciers to re-advance in Patagonia and New Zealand (Moreno et al., 2009; Putnam et al., 2010). In the arid sub-tropical Andes between 20-40°S, it remains unclear as to whether glaciers responded to potential cooling from the south during the ACR and/or enhanced moisture delivery from the north during the YD. Fortunately, updated production rate calibrations for the Central Andes (Kelly et al., 2015; Martin et al., 2015, 2017) now enable accurate calculation of exposure ages with millennial-scale precision, meaning the ACR and YD events can potentially be discriminated. We revisit this topic in Section 5.

# 3. Methods

## 3.1. Dating of moraines at the Sierra de Aconquija

We collected a total of 22 boulder samples from moraine units M1, M2, and M3, and calculated their exposure ages based on measured concentrations of $^{10}$Be produced in situ in quartz. Quartz-rich granite and gneiss boulders at least 1 m in height and exhibiting no obvious signs of surface erosion were sampled from stable moraine crests (Fig. 3). Approximately 750 g were collected from the uppermost 2-3 cm of each boulder with a hammer and chisel. Samples were crushed and sieved to separate the 250-500 µm particle fraction and the magnetic fraction was separated using a Frantz magnetic separator. The non-magnetic fraction was chemically cleaned to isolate grains of quartz. Organic and carbonate material was removed with $H_2O_2$ and HCl, prior to 3 rounds of leaching with a 1% HF, 1% $HNO_3$ mixture (12 hours per round) to dissolve non-quartz minerals and eliminate meteoric $^{10}$Be. This cleaning protocol is similar to that of Kohl and Nishiizumi (1992). Samples were then dissolved in concentrated HF, and Be was isolated using standard column chemistry procedures at the GFZ German Research Centre for Geosciences in Potsdam, Germany (see von Blanckenburg et al., 2004; Wittmann et al., 2016). Each sample received a carrier solution containing 150 µg of $^{9}$Be. The isolated Be was then calcinated and each sample was pressed into a target using a $AgNO_3$ matrix.

Accelerator mass spectrometer (AMS) measurements were performed at the University of Cologne, Germany, and $^{10}$Be/$^{9}$Be ratios were normalised to standards KN01-6-2 and KN01-5-3, with $^{10}$Be/$^{9}$Be ratios of 5.35 $\times10^{-13}$ and 6.32 $\times10^{-12}$, respectively. These ratios are consistent with a $^{10}$Be half-life of 1.36 (±0.07) $\times10^{6}$ yr and the 07KNSTD standardisation (Nishiizumi et

al., 2007), which is recommended when using the CRONUS-Earth (Marrero et al., 2016) and the CREp calculators (Martin et al., 2017). Measured $^{10}Be/^{9}Be$ ratios ranged between 1.95 $\times10^{-13}$ and 2.7 $\times10^{-12}$. To calculate the $^{10}Be$ concentration, a batch-specific blank $^{10}Be/^{9}Be$ ratio of 3.54 $\times10^{-15}$ ($\pm$ 2.96 $\times10^{-15}$, $n$ = 3 blanks) was subtracted from measured isotope ratios to account for $^{10}Be$ background contamination during sample processing. The AMS measurements for the exposure blanks registered only 1-2 $^{10}Be$ counts.

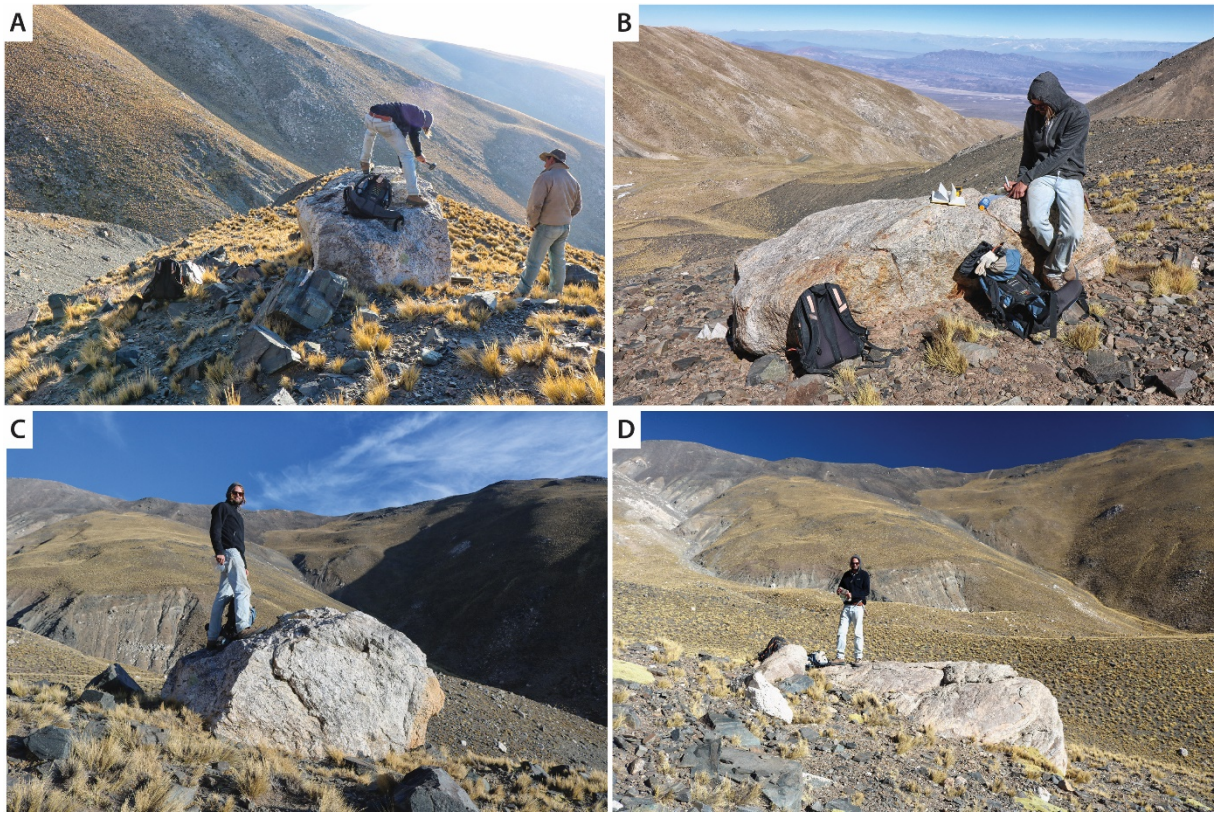


**Fig. 3. (A-C)** Examples of boulders sampled for cosmogenic $^{10}Be$ exposure dating. **(D)** Example of a boulder exhumed from within a moraine crest.

Exposure ages were calculated using the CREp online calculator (Martin et al., 2017; available online at: http://crep.crpg.cnrs-nancy.fr). Corrections were made for topographic shielding and sample thickness (Table 1), and ages were calculated assuming zero surface erosion of boulders and a density of 2.7 g $cm^{-3}$. We used the reference (SLHL) production rate of 3.74 ($\pm$0.09) at $g^{-1}$ $yr^{-1}$ reported for the high-elevation Central Andes by Martin et al. (2015); this rate averages three well-clustered and highly consistent calibration sites in the same region and elevation range (3800-4900 m) as our sample locations (Blard et al., 2013; Kelly et al., 2015; Martin et al., 2015). Other parameters included the Lal/Stone time-corrected scaling scheme (Lal, 1991; Stone, 2000; Balco et al., 2008), the standard atmosphere model (NOAA, 1976),

and the atmospheric $^{10}$Be-based VDM geomagnetic database of Muscheler et al. (2005) and Valet et al. (2005).

From the cluster of boulder exposure ages obtained for each moraine, we selected the oldest of each as being representative of the timing of moraine formation (cf., Putkonen and Swanson, 2003; Zech et al., 2009b). Boulder exposure ages collected from moraines typically exhibit wide dispersion, and simply averaging all measured ages frequently results in a false age of deposition (Ivy-Ochs et al., 2007; Applegate et al., 2010; Kirkbride and Winkler, 2012; Ivy-Ochs and Briner, 2014). Incomplete boulder exposure—resulting from moraine degradation and differential boulder shielding, exhumation, toppling and surface erosion—generates ages that are younger than the true age of a moraine, and is more common than nuclide inheritance in many regions (Putkonen and Swanson, 2003; Hall et al., 2009; Heyman et al., 2011). This tendency to underestimate ages has been demonstrated with large compilations of boulder exposure ages from around the world (Heyman et al., 2011) and numerical analyses (Putkonen and Swanson, 2003), even when tall boulders are preferentially sampled (Heyman et al., 2016). Therefore, unless morphostratigraphic observations support a particular age interpretation, the oldest boulder age within a cluster, after the exclusion of obvious old outliers attributed to prior exposure, is likely to be the closest to the true depositional age of the respective moraine (Zech et al., 2009b; Heyman et al., 2011). This approach has been adopted by many previous studies dating glacial landforms (Briner et al., 2005; Zech et al., 2007a,b; 2009a, 2010; Hall et al., 2009; May et al., 2011). Interested readers are referred to Appendix 1, where we elaborate on this methodological approach and show that using alternative approaches (e.g., mean boulder ages or frequency density plots) do not result in substantial changes to the inferred moraine ages or overall paleoclimate interpretations.

| Valley | Moraine | Sample | Latitude | Longitude | Elevation (m) | Shielding correction | Sample thickness (cm) | $^{10}$Be concentration ($10^5$ at/g) | $^{10}$Be concentration uncertainty ($10^5$ at/g) | Boulder height (m) |
|---|---|---|---|---|---|---|---|---|---|---|
| Río Cerillos valley | M1 | ACON-M1 | - 27.1648 | - 66.0884 | 4359 | 0.980 | 2.5 | 9.638 | 0.366 | 1.0 |
| | | ACON-M2 | - 27.1648 | - 66.0881 | 4369 | 0.980 | 2.5 | 14.890 | 0.473 | 1.2 |
| | | ACON-M3 | - 27.1652 | - 66.0873 | 4404 | 0.980 | 2.5 | 31.433 | 0.986 | 1.4 |
| | | ACON-M4 | - 27.1653 | - 66.0839 | 4489 | 0.980 | 2.5 | 18.964 | 0.610 | 1.0 |
| | | ACON-M5 | - 27.1654 | - 66.0865 | 4429 | 0.980 | 2.5 | 20.503 | 0.658 | 1.1 |
| | | ACON-M6 | - 27.1654 | - 66.0869 | 4420 | 0.980 | 2.5 | 12.298 | 0.410 | 1.0 |
| | M2 | ACON-MB1 | - 27.1633 | - 66.0860 | 4401 | 0.980 | 2.5 | 10.793 | 0.397 | 1.2 |
| | | ACON-MB2 | - 27.1632 | - 66.0865 | 4388 | 0.980 | 2.5 | 9.775 | 0.354 | 1.0 |
| | | ACON-MB3 | - 27.1632 | - 66.0866 | 4367 | 0.980 | 2.5 | 9.292 | 0.312 | 1.2 |
| | | ACON-MB4 | - 27.1628 | - 66.0878 | 4351 | 0.980 | 2.5 | 7.476 | 0.267 | 1.8 |
| | M3 | ACON-MV1 | - 27.1707 | - 66.0852 | 4465 | 0.980 | 2.5 | 5.158 | 0.217 | 1.0 |
| | | ACON-MV2 | - 27.1701 | - 66.0882 | 4397 | 0.975 | 2.5 | 5.022 | 0.193 | 1.1 |
| | | ACON-MV3 | - 27.1702 | - 66.0873 | 4415 | 0.975 | 2.5 | 5.634 | 0.221 | 1.1 |
| | | ACON-MV5 | - 27.1706 | - 66.0860 | 4450 | 0.975 | 2.5 | 5.337 | 0.196 | 1.0 |
| Portal de las Yaretas valley | M3a | YAR03 | - 27.2615 | - 66.1732 | 4210 | 0.970 | 2.0 | 5.348 | 0.203 | 1.6 |
| | | YAR04 | - 27.2615 | - 66.1732 | 4208 | 0.970 | 3.0 | 5.473 | 0.193 | 1.3 |
| | | YAR05 | - 27.2615 | - 66.1731 | 4213 | 0.970 | 3.0 | 4.785 | 0.183 | 1.4 |
| | M3b | YAR07 | - 27.2621 | - 66.1682 | 4400 | 0.970 | 2.0 | 5.482 | 0.211 | 1.0 |
| | | YAR08 | - 27.2630 | - 66.1686 | 4392 | 0.970 | 3.0 | 4.868 | 0.203 | 1.0 |
| | | YAR09 | - 27.2624 | - 66.1697 | 4365 | 0.970 | 2.0 | 5.161 | 0.185 | 1.8 |
| | M3c | YAR-10 | - 27.2598 | - 66.1575 | 4654 | 0.970 | 2.5 | 3.708 | 0.170 | 1.0 |
| | | YAR-11 | - 27.2595 | - 66.1603 | 4593 | 0.970 | 2.5 | 3.919 | 0.182 | 1.4 |

**Table 1.** Sample properties and measured $^{10}$Be data for each boulder dated on the Sierra de Aconquija moraines.

## 3.2. Compilation and recalculation of moraine exposure ages in the Central Andes

We compiled all $^{10}$Be data reported from glacial moraines in the Central Andes north of the study area (Fig. 4; Table 2) to contextualise our moraine exposure age results from the Sierra de Aconquija. These data have been reported from 30 study locations spanning a 20° latitudinal range from 7.0°S (the Cajamarca region of northern Peru; Shakun et al., 2015) to 27.2°S (the Sierra de Aconquija in northwestern Argentina; this study). These sites have a combined total of 160 individual dated moraines, of which 144 represent glacier advances (lateral or terminal moraines) and 16 are recessional moraines (representing a hiatus during retreat, but not a re-advance). The total number of boulders sampled in the compilation is 794, of which 63 (7.9%) were interpreted by the original studies to be anomalously old outliers resulting from nuclide inheritance. In the compilation here, we maintained the interpretation of these particular boulders as outliers attributed to nuclide inheritance, following the original studies. After excluding these outliers due to nuclide inheritance, the mean and median number of remaining sampled boulders per moraine in each age cluster are 4.5 and 3, respectively.

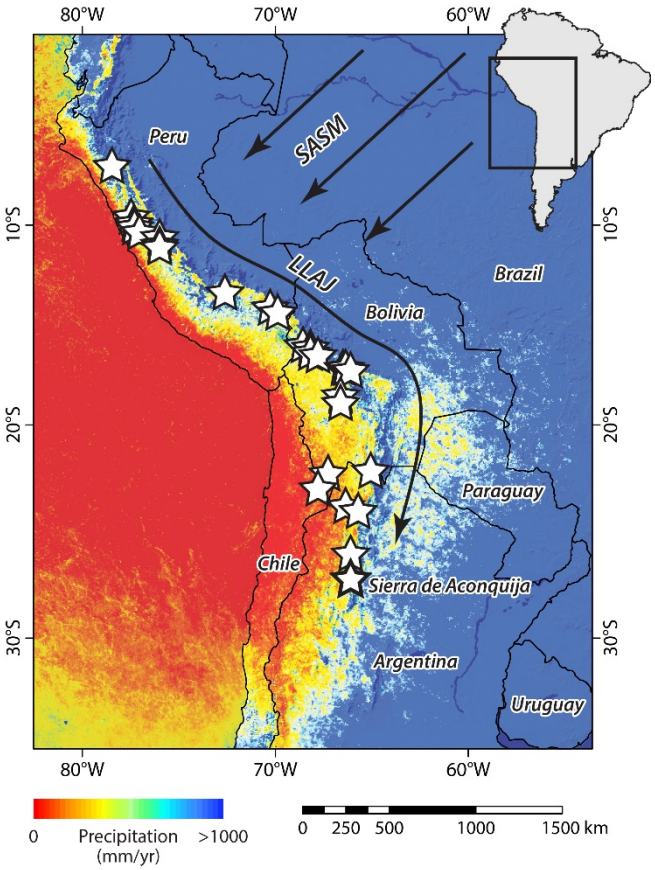


**Fig. 4.** Map of the 30 compiled study sites with dated moraines in the Central Andes (marked with stars), north of the Sierra de Aconquija (marked in bold). See Table 2 for site locations and references to the original studies. Colours indicate annual rainfall rates from TRMM 2B31 (Bookhagen and Strecker, 2008); schematic arrows indicate moisture transport from the northeast during the South American Summer Monsoon (SASM) and via the Low Level Andean Jet (LLAJ).

| Study Site | Country | References | Latitude | Longitude | Mean Elevation (m) | No. boulders |
|---|---|---|---|---|---|---|
| Cajamarca | Peru | Shakun et al. (2015) | - 7.0 | - 78.4 | 3,912 | 30 |
| Northern Cordillera Blanca | Peru | Farber et al. (2005) | - 9.6 | - 77.4 | 3,909 | 49 |
| Queshque Valley | Peru | Stansell et al. (2017); Farber et al. (2005) | - 9.8 | - 77.3 | 4,420 | 31 |
| Cordillera Blanca | Peru | Smith and Rodbell (2010); Glasser et al. (2009) | - 10.0 | - 77.3 | 4,348 | 78 |
| Cordillera Huayhuash | Peru | Hall et al. (2009) | - 10.2 | - 76.9 | 4,184 | 60 |
| Nevado Huaguruncho | Peru | Stansell et al. (2015) | - 10.6 | - 75.9 | 4,362 | 48 |
| Collpa Valley | Peru | Smith et al. (2005a); Smith et al. (2005b) | - 10.9 | - 75.9 | 4,173 | 6 |
| Calcalcocha Valley | Peru | Smith et al. (2005a); Smith et al. (2005b) | - 11.0 | - 76.0 | 4,259 | 26 |
| Antacocha Valley | Peru | Smith et al. (2005a); Smith et al. (2005b) | - 11.0 | - 76.0 | 4,255 | 22 |
| Alcacocha Valley | Peru | Smith et al. (2005a); Smith et al. (2005b) | - 11.1 | - 76.0 | 4,333 | 91 |
| Cordillera Vilcabamba | Peru | Licciardi et al. (2009) | - 13.4 | - 72.5 | 4,307 | 28 |
| Cordillera Carabaya - Quebrada Tirataña | Peru | Bromley et al. (2016) | - 14.2 | - 70.3 | 4,583 | 4 |
| Cordillera Carabaya - Laguna Aricoma | Peru | Bromley et al. (2016) | - 14.3 | - 69.8 | 4,712 | 8 |
| Illampu Massif - San Francisco Valley | Bolivia | Zech et al. (2007b) | - 16.0 | - 68.5 | 4,625 | 12 |
| Zongo Valley | Bolivia | Smith et al. (2005a); Smith et al. (2005b) | - 16.1 | - 68.2 | 3,675 | 24 |
| Cordillera Real, Telata moraines | Bolivia | Jomelli et al. (2011) | - 16.3 | - 68.1 | 4,605 | 59 |
| Milluni Valley | Bolivia | Smith et al. (2005a); Smith et al. (2005b) | - 16.4 | - 68.2 | 4,604 | 18 |
| Nevado Illimani | Bolivia | Smith et al. (2011) | - 16.6 | - 67.8 | 4,352 | 22 |
| Cordillera Cochabamba - Huara Loma Valley | Bolivia | May et al. (2011); Zech et al. (2007b) | - 17.2 | - 66.3 | 4,196 | 24 |
| Cordillera Cochabamba - Rio Suturi Valley | Bolivia | Zech et al. (2007b) | - 17.2 | - 66.5 | 3,912 | 8 |
| Cordillera Cochabamba - Wara Wara Valley | Bolivia | Zech et al. (2010) | - 17.3 | - 66.1 | 4,179 | 10 |
| Cerro Azanaques | Bolivia | Martin et al. (2018) | - 18.9 | - 66.7 | 4,366 | 6 |
| Cerro Tambo | Bolivia | Martin et al. (2018) | - 19.8 | - 66.6 | 4,191 | 6 |
| Tres Lagunas | Argentina | Zech et al. (2009a) | - 22.2 | - 65.1 | 4,426 | 35 |
| Uturuncu Volcano | Bolivia | Blard et al. (2014) | - 22.3 | - 67.2 | 4,827 | 6 |
| Chajnantor Plateau | Chile | Ward et al. (2015) | - 23.0 | - 67.8 | 4,740 | 12 |
| Nevado de Chañi | Argentina | Martini et al. (2017) | - 24.0 | - 65.7 | 4,553 | 43 |
| Quevar Volcano | Argentina | Luna et al. (2018) | - 24.4 | - 66.8 | 4,663 | 11 |
| Sierra de Quilmes | Argentina | Zech et al. (2017) | - 26.2 | - 66.2 | 4,303 | 11 |
| Sierra de Aconquija | Argentina | This study | - 27.2 | - 66.1 | 4,397 | 22 |

**Table 2.** Study sites compiled in the Central Andes where moraine ages have been determined by $^{10}$Be cosmogenic nuclide exposure dating of surface boulders.

We re-calculated all $^{10}$Be-derived boulder exposure ages using the regional production rate and other parameters recommended by Martin et al. (2015) and described in Section 3.1. We did not extend the compilation farther south for two reasons: (i) the production rate and age calculation parameters reported by Martin et al. (2015) may not be appropriate farther south and could result in incorrect ages in the mid-latitudes and Patagonia, and (ii) we are primarily interested in reconstructing the response of Central Andean glaciers to fluctuations in the SASM (Fig. 4). All sites with dated moraines south of the Sierra de Aconquija (e.g., Zech et al., 2006; 2007a; Moreiras et al., 2017; Terrizzano et al., 2017) are situated on the western flank of the Andes, where moisture is sourced from the Pacific westerlies. While it would be worthwhile to review how fluctuations in the Pacific westerlies influenced glaciers in the Southern Andes, this consideration lies beyond the scope of the present study. The Sierra de Aconquija (27°S) is the southern-most site with dated moraines located on the eastern margin of the Central Andes to which moisture is predominantly delivered by the SASM.

Previous compilations of moraine ages in the Central Andes have updated boulder ages as new production rate calibrations have been reported (e.g., Rodbell et al., 2009; Jomelli et al., 2014; Ward et al., 2015). However, different studies have taken different approaches to interpreting clusters of boulder ages, and a consistent approach is required to ensure a fair comparison among study sites. For the reasons outlined in Section 3.1, many studies take the oldest boulder age—within a cluster of boulder ages for a given moraine and after the exclusion of outliers attributed to nuclide inheritance— to be the closest to the timing of the glacier advance (e.g., Zech et al., 2006, 2007a,b, 2009b, 2010; 2017; Hall et al., 2009; May et al., 2011). On the contrary, some studies instead (i) calculate mean values of all boulder ages collected on a moraine (Licciardi et al., 2009; Shakun et al., 2015b; Stansell et al., 2015, 2017; Bromley et al., 2016; Martini et al., 2017); (ii) calculate average boulder ages using frequency density plots (Smith and Rodbell, 2010; Jomelli et al., 2011; Smith et al., 2011; Ward et al., 2015); (iii) organise ages chronologically and take the plateau or modal age (Smith et al., 2005a,b) or (iv) combine these various approaches (Terrizzano et al., 2017). As our results for the Sierra de Aconquija demonstrate (see Section 4.1), these different approaches could, in some cases, result in substantially different moraine ages (and consequently palaeoclimate interpretations) for an identical set of boulder ages.

We adopted a uniform strategy for interpreting clusters of boulder ages on moraines—the 'oldest clustered boulder age' approach (see Appendix 1). After eliminating older outliers due to inheritance (in agreement with the original studies), we selected the oldest age within a

cluster of boulder ages as closest to the timing of moraine formation (cf., Putkonen and Swanson, 2003; Briner et al., 2005; Zech et al., 2009b; Heyman et al., 2011; Ivy-Ochs and Briner, 2014). Appendix 1 compares this approach with alternative methods of inferring moraine ages (i.e., mean boulder ages or peaks of boulder age frequency distributions), and reveals that the choice of methodology does not fundamentally change the resulting palaeoclimate interpretations of this study.

# 4. Results

## 4.1. Ages of the Sierra de Aconquija moraines

We determined 22 boulder exposure ages for moraine units M1, M2, and M3 (see Table 3, Fig. 5a). The oldest, M1, is preserved as a lateral moraine in the Río Cerrillos valley, from which the six boulder exposure ages obtained range from 20.3 ±0.8 ka to 62.5 ±2.5 ka. The oldest age is significantly older than the others, so we interpret it to be an outlier resulting from nuclide inheritance. Of the remaining five boulder ages, the oldest is 40.1 ±1.0 ka, which is most likely to be the approximate formation age of M1 (see Section 3). Four boulder exposure ages were collected from lateral moraine M2 in the Río Cerrillos valley; this moraine is inset into M1 and must therefore be younger. The ages obtained are well-clustered and range from 16.4 ±0.6 ka to 22.1 ±0.9 ka.

The youngest moraine unit (M3) was sampled as a lateral moraine cross-cutting M1 and M2 in the Río Cerrillos valley, and as a sequence of end-moraines in the Portal de las Yaretas valley (Fig. 2). In the Río Cerrillos valley, four well-clustered boulder exposure ages were obtained between 11.3 ±0.5 ka and 12.5 ±0.5 ka. In the Portal de las Yaretas valley, three different end moraine crests were sampled. Three boulder exposure ages were determined from the lowermost (M3a), ranging from 11.9 ±0.5 ka to 13.5 ±0.5 ka. Crest M3b is situated ~500 m up-valley, from which three boulder exposure ages range from 11.2 ±0.5 ka to 12.3 ±0.5 ka. Finally, we sampled two boulders on a younger end moraine a further ~1 km up-valley (M3c) with exposure ages of 7.9 ±0.2 ka and 8.5 ±0.2 ka.

All boulder ages are plotted in Fig. 5a and compared with selected palaeoclimate records, which are discussed in Section 5.2.

| Valley | Moraine | Sample | Age (ka) | Uncertainty, 1σ (ka) |
|---|---|---|---|---|
| Río Cerrillos valley | M1 | ACON-M1 | 20.3 | 0.8 |
| | | ACON-M2 | 30.6 | 1.4 |
| | | ACON-M3† | 62.5 | 2.5 |
| | | ACON-M4 | 37.0 | 1.3 |
| | | ACON-M5* | 40.1 | 1.0 |
| | | ACON-M6 | 25.2 | 1.0 |
| | M2 | ACON-MB1* | 22.1 | 0.9 |
| | | ACON-MB2 | 20.3 | 0.7 |
| | | ACON-MB3 | 19.6 | 0.7 |
| | | ACON-MB4 | 16.4 | 0.6 |
| | M3 | ACON-MV1 | 11.3 | 0.5 |
| | | ACON-MV2 | 11.4 | 0.4 |
| | | ACON-MV3* | 12.5 | 0.5 |
| | | ACON-MV5 | 11.7 | 0.5 |
| Portal de las Yaretas valley | M3a | YAR03 | 13.1 | 0.6 |
| | | YAR04* | 13.5 | 0.5 |
| | | YAR05 | 11.9 | 0.5 |
| | M3b | YAR07* | 12.3 | 0.5 |
| | | YAR08 | 11.2 | 0.5 |
| | | YAR09 | 11.8 | 0.5 |
| | M3c | YAR-10 | 7.9 | 0.3 |
| | | YAR-11* | 8.5 | 0.4 |

**Table 3.** Calculated exposure ages for each boulder sampled. Ages were calculated using the CREp online calculator; parameters are given in the Section 3. Reported uncertainties account for uncertainty in measured $^{10}$Be concentrations (Table 2) and uncertainties associated with the $^{10}$Be production rate (Martin et al., 2017).

†Inferred outlier due to nuclide inheritance.

*Oldest sample within the age cluster.

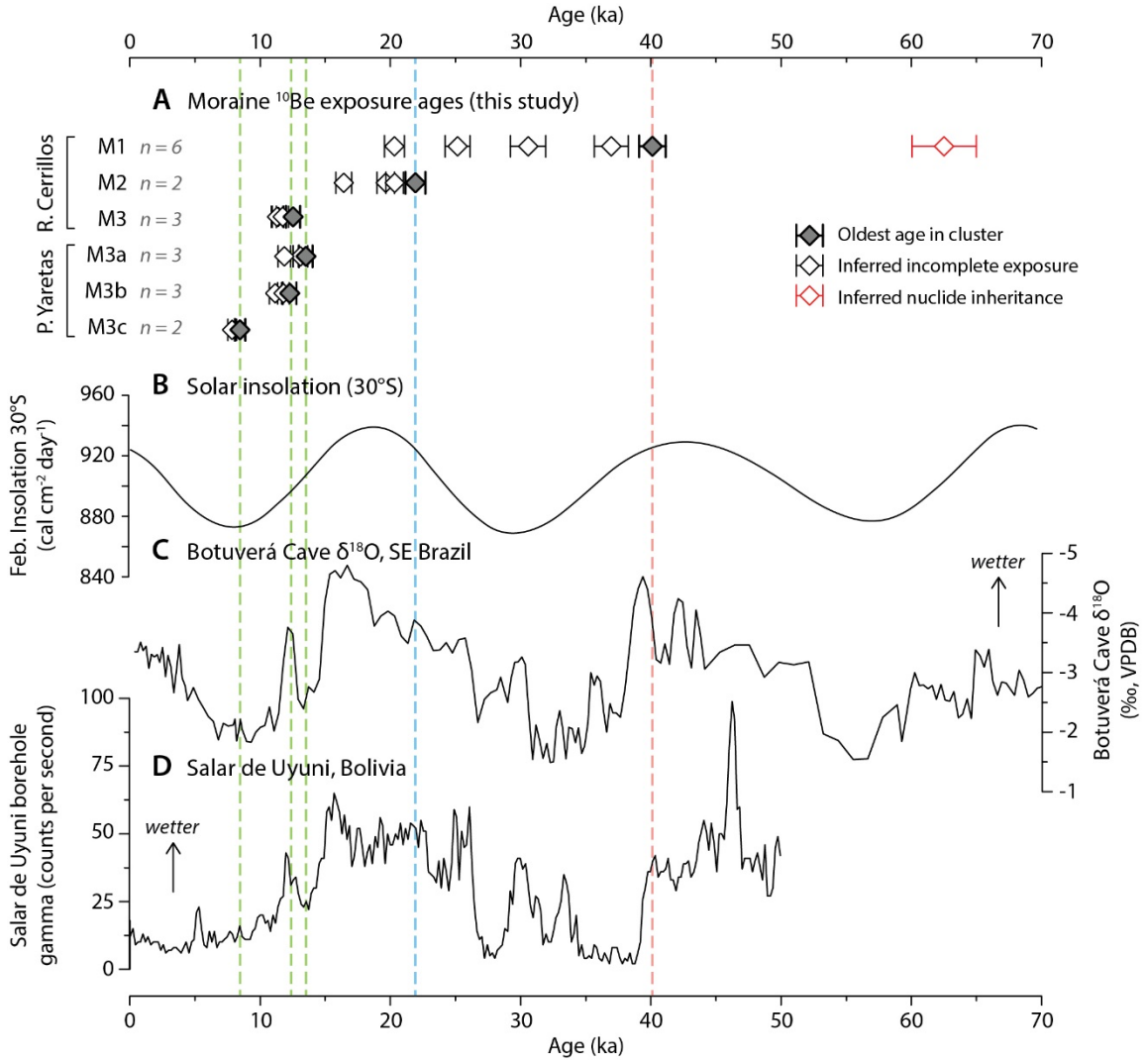


**Fig. 5. (A)** Boulder exposure ages measured for the Sierra de Aconquija moraines, compared with **(B)** solar insolation in February at 30°S (Berger and Loutre, 1991), **(C)** the BTV-3a Botuverá Cave $\delta^{18}O$ record in southeastern Brazil (Wang et al., 2007), and **(D)** gamma counts obtained from a lacustrine core at the Salar de Uyuni, Bolivia (Baker et al., 2001).

## 4.2. Compilation of other moraine ages in the Central Andes

We compiled and re-calculated all previously-reported boulder ages for 160 moraines distributed across the Central Andes (Fig. 4, Table 2). Of these, 144 moraines represent glacier advances (lateral or terminal moraines), the ages of which are plotted as a function of latitude in Fig. 6, focusing on the last 60 kyr. Each point indicates the oldest boulder exposure age sampled on a given moraine, excluding outliers due to nuclide inheritance, and with error bars indicating the ±1σ uncertainty on the respective boulder age. The colour/symbol used for each

point indicates how many individual boulders with clustered ages were sampled on each moraine (again, excluding outliers due to nuclide inheritance).

The moraine ages are distributed across latitude and time. In the northern Central Andes (e.g., the Peruvian Andes at ~10°S) there is a dense spread of moraines dating between 11 ka and 30 ka, as well as a cluster of older (~40 ka), and several younger (Holocene and Little Ice Age) moraines. In the middle sector of the Central Andes (15-20°S), the main cluster of ages lies between 11 ka and 23 ka. In the southern Central Andes, south of ~22.5°S, the ages are more sparsely distributed, but none are younger than 12.5 ka. The clusters of ages are in good agreement with earlier efforts to compile moraine ages in the region (Rodbell et al., 2009; Zech et al., 2009b). Notably, the patterns in the data differ depending on how many boulders are sampled per moraine. If only those moraines with 5 or 6+ clustered boulder ages are considered (marked respectively with purple squares and black stars), there is a clear cross-latitude cluster of ages at 40 ka and a second broader cross-latitude cluster that spans from 11 ka to 30 ka at 10°S and narrows to 15 ka to 25 ka by 25°S, with the oldest age decreasing linearly with latitude. When moraines with fewer dated boulders are considered, these patterns become less clear.

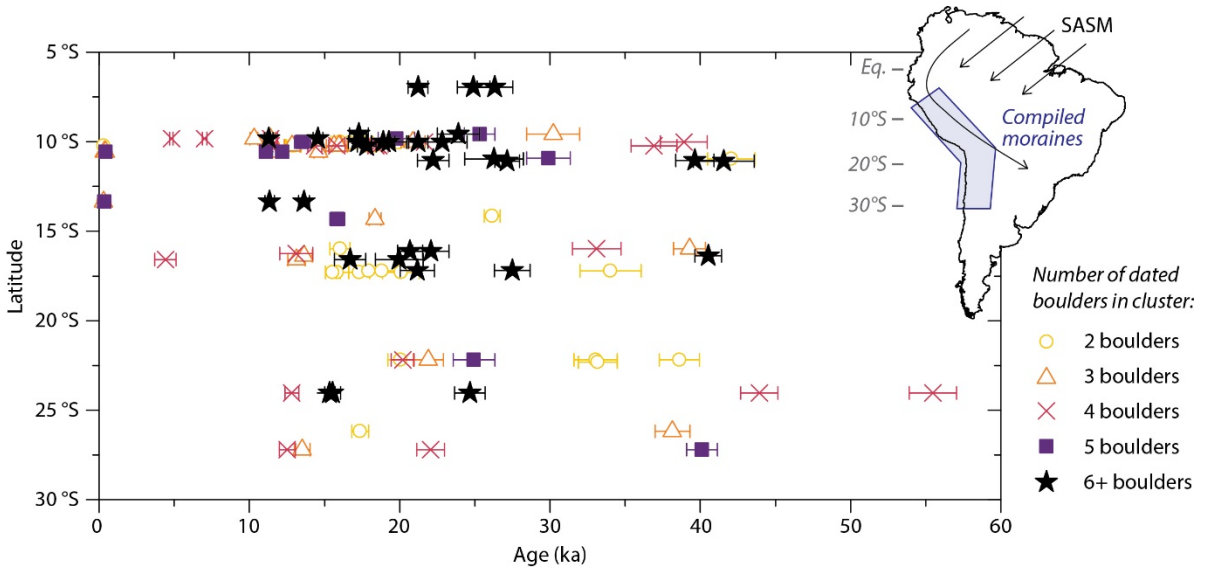


**Fig. 6.** Compilation of all dated moraines in the Central Andes between 5°S and the Sierra de Aconquija at 27°S. Ages were calculated using the CREp calculator and parameters recommended by Martin et al. (2015), and re-interpreted using the 'oldest boulder' approach (see text for details). Each point represents one moraine and is coloured according to the number of clustered boulder ages reported for that moraine, with ±1σ error bars.

How many boulder ages are sufficient to obtain an accurate moraine age? Clearly, the more boulders that are sampled, the closer the oldest age in the cluster is likely to be to the timing of moraine formation (Putkonen and Swanson, 2003; Briner et al., 2005; Heyman et al., 2011). The moraine ages in Fig. 6 that are based on a larger cluster of boulder ages are less likely to change if additional boulders were dated, whereas those derived from a small number of boulder ages (e.g., two or three) are more likely to underestimate the true moraine age. Putkonen and Swanson (2003) quantified this sensitivity using a global data set of boulder ages collected from moraines and a numerical model of moraine diffusion. They estimated the number of boulder ages required, depending on moraine age and initial height, such that the oldest age in the cluster is ≥90% of the age of moraine formation with a 95% probability (Table 4).

| Moraine age (ka) | Initial moraine height (m) | | | | | |
|---|---|---|---|---|---|---|
| | 100 | 80 | 60 | 40 | 30 | 20 |
| 60 | 7 | 7 | 7 | 6 | 5 | 4 |
| 40 | 6 | 6 | 6 | 6 | 5 | 4 |
| 20 | 5 | 5 | 5 | 5 | 5 | 4 |

**Table 4.** The number of boulder ages required from a moraine surface, as a function of moraine age and initial height, such that there is a 95% probability that the oldest age is ≥90% of the age of moraine formation (from Putkonen and Swanson, 2003).

For a 20 ka moraine with an initial height of 20 m, four boulders are required to achieve this level of accuracy and probability. This requirement increases to five boulders if the initial moraine height was 40 m or greater. For a 40 ka moraine, six boulders are required if the initial relief was 40 m or greater. The findings of Putkonen and Swanson (2003) indicate that, of all the moraines dated in the Central Andes and compiled here, many sites have an insufficient number of boulder ages for the oldest clustered age to be within 90% of the true moraine age. Of the 144 moraines representing glacier advances, 77 (i.e., 53%) meet the criterion of four or more boulder ages, 56 moraines (39%) contain five or more boulder ages, and 41 moraines (28%) contain six or more boulder ages. In total, approximately half of the dated moraines in the Central Andes probably do not have the necessary number of boulder ages to provide an accurate estimate of the timing of glacier advance. In Fig. 6, the moraine ages with only two or three boulders (marked with yellow circles and orange triangles) are likely to be under-estimated. The moraines with four boulders (marked with red crosses) are likely to be more accurate, particularly for the younger moraine units, and the majority of the moraine ages with 5 or 6+ boulders (marked with purple squares and black stars) are likely to be more than 90% of the true moraine age. This inference based on modelling is in agreement with the improved clustering of ages (e.g., around 40 ka) and the emergence of spatial patterns (e.g., the linear

latitude/age relationship between ~25-30 ka) among the sites with only 5 or 6+ boulders per moraine. Additional evidence in support of this approach is given in Appendix 1.

There are fewer data points (11 moraines) with ages older than 60 ka (Fig. 7), although many are based on five or more boulder ages. The majority of the data lie in the Peruvian Andes at ~10°S (Smith et al., 2005a,b) and the oldest moraine (~330 ka) is in the Alcacocha valley in Peru (Smith et al., 2005a,b). There are two moraines with similar ages of ~207 ka and ~209 ka at 11°S and 22°S, respectively. Five moraine ages in the Peruvian Andes are distributed at even intervals between 207 ka and 313 ka, i.e., every ~21 kyr on average.

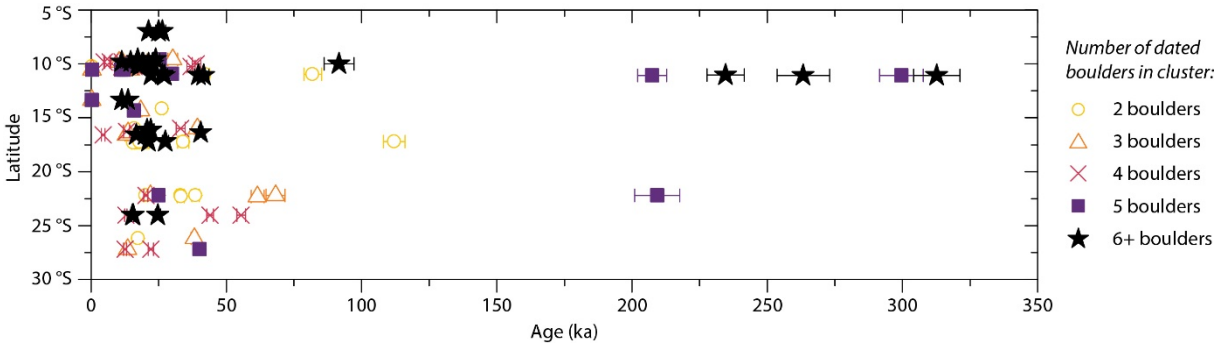


**Fig. 7.** Compilation of dated moraines in the Central Andes as per Fig. 6, but extending back to 350 ka.

# 5. Discussion

## 5.1. Timing of glaciations at the Sierra de Aconquija (27°S)

### *5.1.1. Moraine unit M1*

The age of M1 indicates that there was a glacier advance at ~40 ka, which is the largest advance recorded on the Sierra de Aconquija (Fig. 2). This advance occurred at approximately the summer insolation maximum in the southern sub-tropics (Fig. 5b), when the SASM was intensified and conditions in the Central Andes were wetter (the Minchin pluvial phase), the Botuverá Cave $\delta^{18}O$ record indicates greater depletion, and lakes on the Altiplano and Puna plateaus were deeper and fresher (Fig. 5). Glaciers advanced in nearby parts of the southern Central Andes around this time, for example the Nevado de Chañi (24°S; Martini et al., 2017) and the Sierra de Quilmes (26°S; Zech et al., 2017), as well as farther north at the Chajnantor plateau (23°S; Ward et al., 2015; 2017), Uturuncu volcano (22°S; Blard et al., 2014; Ward et al., 2017), and the Cordillera Huayhuash in Peru (10°S; Hall et al., 2009). We therefore infer that the M1 advance at the Sierra de Aconquija occurred within a more widespread wet period

in the Central Andes, corresponding to the summer insolation maximum around 40-45 ka, during which the SASM was intensified. A lack of terrestrial palaeo-temperature reconstructions from this time (Baker and Fritz, 2015) makes it difficult to know whether this was also a time of especially cold temperatures and whether cooling was simultaneously needed to trigger the advance of Central Andean glaciers. Nonetheless, these new results from the Sierra de Aconquija provide new evidence that glaciers in the Central Andes advanced in phase with intensification of the SASM during summer insolation maxima, at least as far south as 27°S in northwestern Argentina.

It is worth noting the ~62.5 ka boulder outlier on the M1 moraine. We interpret this age to result from nuclide inheritance; this could be due to prior exposure of the boulder on a hillslope before it was incorporated into the moraine. However, the boulder might also have been incorporated from a pre-existing moraine. This scenario is not unlikely given that the M1 moraines occupy the full width of the valleys (Fig. 2), so they must have eroded or incorporated any pre-existing moraine deposits. If this age were derived from an older moraine in the Río Cerrillos valley, it might have corresponded with the summer insolation maximum at ~65-70 ka (Fig. 5b). This interpretation remains speculative, because there is no cluster of ages or a mapped moraine unit pre-dating M1. Nonetheless, moraines of this age have been reported elsewhere in the southern Central Andes including the Sierra de Santa Victoria (22°S; Zech et al., 2009a) and Uturuncu volcano (22°S; Blard et al., 2014). We speculate that older advances may also have coincided with insolation maxima, although evidence of earlier glaciations at the Sierra de Aconquija has been overprinted by M1, M2, and M3. Indications of precessional periodicity in even older moraine ages (Fig. 7) support this interpretation.

### *5.1.2. Moraine unit M2*

Our estimated age for M2 (~22 ka) lies within the global LGM and just before the summer insolation peak in the southern hemisphere sub-tropics at ~20 ka. This period was marked by deep and fresh Altiplano lakes (Baker et al., 2001; Baker and Fritz, 2015) and other palaeoclimate records that indicate wet conditions throughout the Central Andes at this time (see Section 2.2). Many other moraines in the Central Andes have been dated to ~20-25 ka; we refer to Section 5.3 and the supplementary material for a compilation of these ages. As with the earlier insolation peak around 40-45 ka, this was a time of enhanced moisture flux to the Central Andes, most likely due to southward displacement of the ITCZ in the tropical Atlantic and intensification of the SASM. The LGM was also a time of cooler temperatures. Glacier mass balance modelling in the Bolivian Andes (Kull et al., 2008) and TEX-86 palaeothermometry in sediments from Lake Titicaca (Fornace et al., 2011; Baker and Fritz,

2015) both suggest that the LGM was ~6°C colder in the tropical/sub-tropical Andes than it is today.

We interpret that the M2 advance at the Sierra de Aconquija occurred at ~22 ka due to increased precipitation amounts during a period of cold temperatures. We expand on this interpretation in Section 5.3, in which we discuss the compilation of moraine ages for the entire Central Andes. As with the M1 moraines, the ages of the M2 moraines from the Sierra de Aconquija also provide evidence that glacier advances in the southern Central Andes occurred in phase with wet intervals associated with insolation maxima (Fig. 5).

### *5.1.3. Moraine unit M3*

The ages of the M3 moraines (Fig. 8a) are especially important for discerning how the Younger Dryas (YD) and the Antarctic Cold Reversal (ACR) influenced glaciers in the sub-tropical Andes. Here, we examine the late glacial period, in which the ages of the four sampled M3 moraines are compared with $\delta^{18}O$ curves obtained from ice cores in West Antarctica and Greenland (Fig. 8b), as well as the Botuverá Cave $\delta^{18}O$ record (Fig. 8c). The two polar records are predominantly temperature proxies, and illustrate anti-phased behaviour between the Northern and Southern hemispheres during deglaciation, with the ACR (the dominant event in the Southern Hemisphere) preceding the YD (the dominant event in the northern hemisphere) (Putnam et al., 2010; Pedro et al., 2011, 2016). The terrestrial Botuverá Cave speleothem $\delta^{18}O$ record is primarily a proxy for precipitation and the intensity of the SASM in sub-tropical South America (Cruz et al., 2005; Wang et al., 2007). It is highly correlated with the Greenland $\delta^{18}O$ record because cold events in the North Atlantic displace the ITCZ southward, leading to warming of sea surface temperatures in the tropical Atlantic and intensification of the SASM (see Section 2.2). Therefore, glacier advances in the Central Andes could have resulted from cooling of the Southern Hemisphere during the ACR, an increase in precipitation due to intensification of the SASM during the YD, or both; this issue remains contentious (Jomelli et al., 2014; Ward et al., 2015).

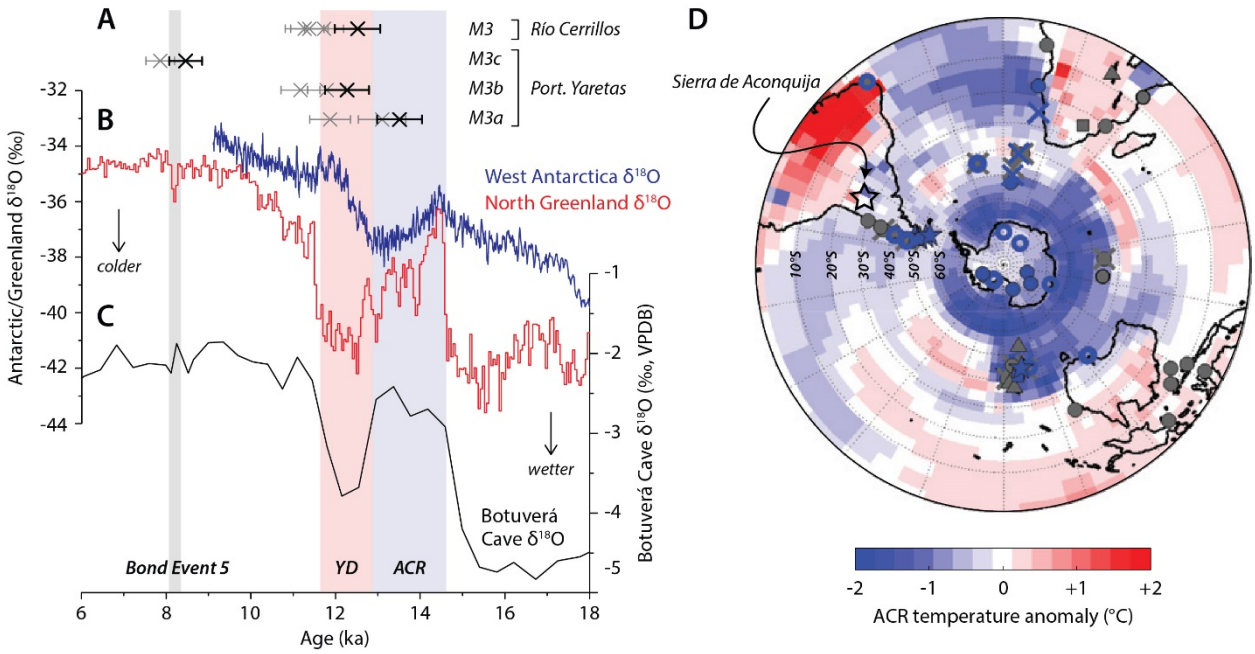


**Fig. 8. (A)** Boulder ages measured on each of the M3 moraines at the Sierra de Aconquija (the oldest boulder in each cluster is black, while the others are grey), compared with **(B)** $\delta^{18}O$ series obtained from ice cores in West Antarctica (core WDC 6A-7; WAIS Divide Project Members, 2013) and Greenland (NGRIP; North Greenland Ice Core Project Group Members, 2004) (left axis); as well as **(C)** the BTV-3a Botuverá Cave $\delta^{18}O$ record (Wang et al., 2007) (right axis). **(D)** This figure has been reproduced from Pedro et al. (2016) and shows their simulation of Southern Hemisphere temperature anomalies during the Antarctic Cold Reversal.

The oldest boulder age obtained for the lowermost end moraine in the Portal de las Yaretas valley (M3a; 13.5 ±0.5 ka) coincides with the ACR. Three boulders were sampled on M3a (Fig. 2b), the youngest of which cannot be correct because it would make the moraine younger than M3b, which is morphologically impossible. Even if the older two boulder ages were averaged, M3a would still coincide with the ACR. The M3a moraine could be a terminal moraine (i.e., the glacier was previously smaller and advanced to this position during the ACR), or a recessional moraine (i.e., the glacier was previously larger and M3a represents a hiatus during its retreat that coincided with the ACR). The M3 moraines in the Río Cerrillos valley (Fig. 2a) exhibit an identical morphological expression, with end moraines ~500 m up-valley from the lowermost exposed M3 deposits. Although we did not sample the lowermost deposits in the Río Cerrillos valley, we interpret them to be equivalent to M3a in the Portal de las Yaretas valley. Therefore, we infer that the outermost mapped extents of the M3 moraines were formed at ~13.5 ka. As the M3 moraines clearly overprint M2, we interpret our data to indicate a glacier advance (i.e.,

making M3a a terminal moraine) during the ACR, and therefore driven by cooling of the Southern Hemisphere.

The results of a transient simulation of Southern Hemisphere temperature anomalies during the ACR by Pedro et al. (2016) is depicted in Fig. 8d. This record was generated using the Community Climate System Model v.3 *TraCE* simulation sensitivity experiment *EXP-ACR* (Liu et al., 2009; He et al., 2013), and the temperature anomaly was calculated as the mean temperature for the entire ACR minus the mean temperature during the 50 years before the onset of the ACR. This map therefore shows the simulated spatial reach of ACR cooling in the Southern Hemisphere. Pedro et al. (2016) compared these model results with palaeoclimate records, shown as symbols in Fig. 8b and coloured blue if they register a signal of ACR cooling, or grey if the presence of an ACR signal is ambiguous. In South America, as well as on other continents, existing palaeoclimate records show a clear response to the ACR at latitudes south of 40°S. Between 20°S and 40°S the presence of an ACR signal is unclear in existing proxies/archives, despite the palaeoclimate simulation predicting that temperatures might have cooled as far north as ~25°S. Therefore, a glacier advance concurrent with the ACR at the Sierra de Aconquija (marked with a star in Fig. 8b) is important evidence in support of the simulation by Pedro et al. (2016) and suggests that cooling during the ACR did indeed occur as far north as 27°S in South America.

The YD is also represented in the Sierra de Aconquija moraine record. Four ages were obtained for the lateral M3 moraine in the Río Cerrillos valley, the oldest of which (12.5 ±0.5 ka) corresponds to the YD. An average of all the sampled ages would still coincide with the YD. Similarly, the age of the M3b moraine sampled in the Portal de las Yaretas valley also coincides with the YD (12.3 ±0.5 ka). As stated previously, the M3b surfaces have end moraines situated ~500 m up-valley from the M3a deposits in both of the sampled catchments (Fig. 2), indicating a similar history of glacier dynamics at both sites. We infer that the M3 glaciers were retreating after the ACR, within the long-term warming trend of global deglaciation, but that the M3b moraines represent a brief hiatus during retreat and a small re-advance at ~12.3-12.5 ka. As this small re-advance coincides with the YD, we interpret that it occurred in response to enhanced monsoonal moisture transport to the Sierra de Aconquija, as the SASM is known to have been strengthened during the YD interval (see Section 2.2).

Finally, the age of the uppermost M3c end moraine in the Portal de las Yaretas valley (Fig. 2b) coincides with Bond Event 5 (Bond et al., 1997), also known as the 8.2 ka event. Like the YD, the 8.2 ka event was a cold event in the North Atlantic and is recorded by a negative $\delta^{18}O$ excursion in Greenland (Fig. 8b) and a decrease in North Atlantic temperatures of 1.5-3.0°C (Alley et al., 1997; Barber et al., 1999; Thomas et al., 2007). It has been suggested that the 8.2 ka event occurred within a longer period of cooling starting at 8.6 ka and lasting up to 600

years (Rohling and Pälike, 2005). A southward shift of the tropical Atlantic summer ITCZ position between 7.8 ka and 8.4 ka has also been identified from sedimentary deposits in the Cariaco Basin (Haug et al., 2001; Rohling and Pälike, 2005), and lacustrine sedimentary cores indicate wet conditions in the Central Andes at exactly this time (Tiner et al., 2018). Jomelli et al. (2011) similarly identified a recessional moraine unit in the high Zongo valley of the Cordillera Real, Bolivia (16°S), with an age of 8.5 ±0.4 ka. Therefore, we interpret the M3c moraine age to coincide with Bond Event 5, representing a short-lived pause in glacier retreat due to intensification of the SASM and a corresponding increase in moisture delivered to the Sierra de Aconquija. This interpretation invokes an equivalent coupling between the tropical Atlantic and the SASM noted for the M3b/YD advance, only smaller in magnitude, which is consistent with the shorter length of the M3c glacier in the Portal de las Yaretas valley.

The Sierra de Aconquija occupies a portion of the southern Central Andes that is especially sensitive to climate change; it is far enough south to register the ACR and far enough north to register fluctuations in the intensity of the SASM. Glaciers on the range responded to both the YD and the ACR, as well as Bond Event 5 during the Holocene. Colder temperatures during the ACR probably explain the outermost M3a positions followed by glacier retreat, as temperatures subsequently warmed. The retreat was seemingly interrupted during both the YD and the Bond Event 5, most likely as a result of intensification of the SASM. The Sierra de Aconquija is located at the southern-most limit of the LLAJ today (Fig. 1a); our findings indicate that at this latitude, brief intensification of the SASM was sufficient to pause glacier retreat, but insufficient to cause major re-advances. Consequently, we interpret this location to be approximately the most southerly latitude where a short-lived increase in precipitation related to the YD can be detected in moraine records along the eastern flanks of the Central Andes.

## 5.2. Compilation of moraine ages across the Central Andes

Our compilation of moraine ages for the Central Andes is the first to uniformly take the oldest boulder from clustered boulder ages to be the closest in age to the true timing of moraine formation, while also updating boulder exposure ages with the latest cosmogenic nuclide production rate constraints. The ‘oldest clustered boulder age’ approach recognises that the moraine ages reported across the Central Andes vary in their accuracy, and that at least half probably underestimate the timing of advances as a result of too few boulders having been sampled. Therefore, simply plotting all measured moraine ages (Fig. 6) generates a complicated picture that combines ages of varying probable accuracy.

We re-plot the compilation of moraine ages from Fig. 6 for the 0-60 ka time period in Fig. 9. To focus on the spatial patterns in timing, the data are binned by latitude and age. By binning the

data, we assume that moraine ages in individual valleys are correlatable and representative of that latitude more generally. We used 5° bins for latitude, and variable bin sizes for age (0.5 ka between 0 ka and 10 ka; 1 ka between 10 ka and 20 ka; 2 ka between 20 ka and 40 ka; 4 ka between 40 ka and 60 ka), reflecting the increase in age uncertainty with increasing age (see supplementary material). In panels D, E, and F, we repeat the plot using data from moraines that have six or more boulders, five or more boulders, and four or more boulders, respectively. There is a trade-off between the accuracy of the ages and the number of moraines that can be included, but all three plots are likely to be reasonable reconstructions of when glaciers advanced (see Section 4.2). For comparison, panels A-C show a range of palaeoclimate proxies, including a $^{231}Pa/^{230}Th$ proxy for the strength of the Atlantic Meridional Overturning Circulation (AMOC), atmospheric $CO_2$, sea surface temperatures from the northern coast of South America, and the average temperature for the entire Southern Hemisphere during the period of global deglaciation. Millennial-scale climate events are marked with grey bars.

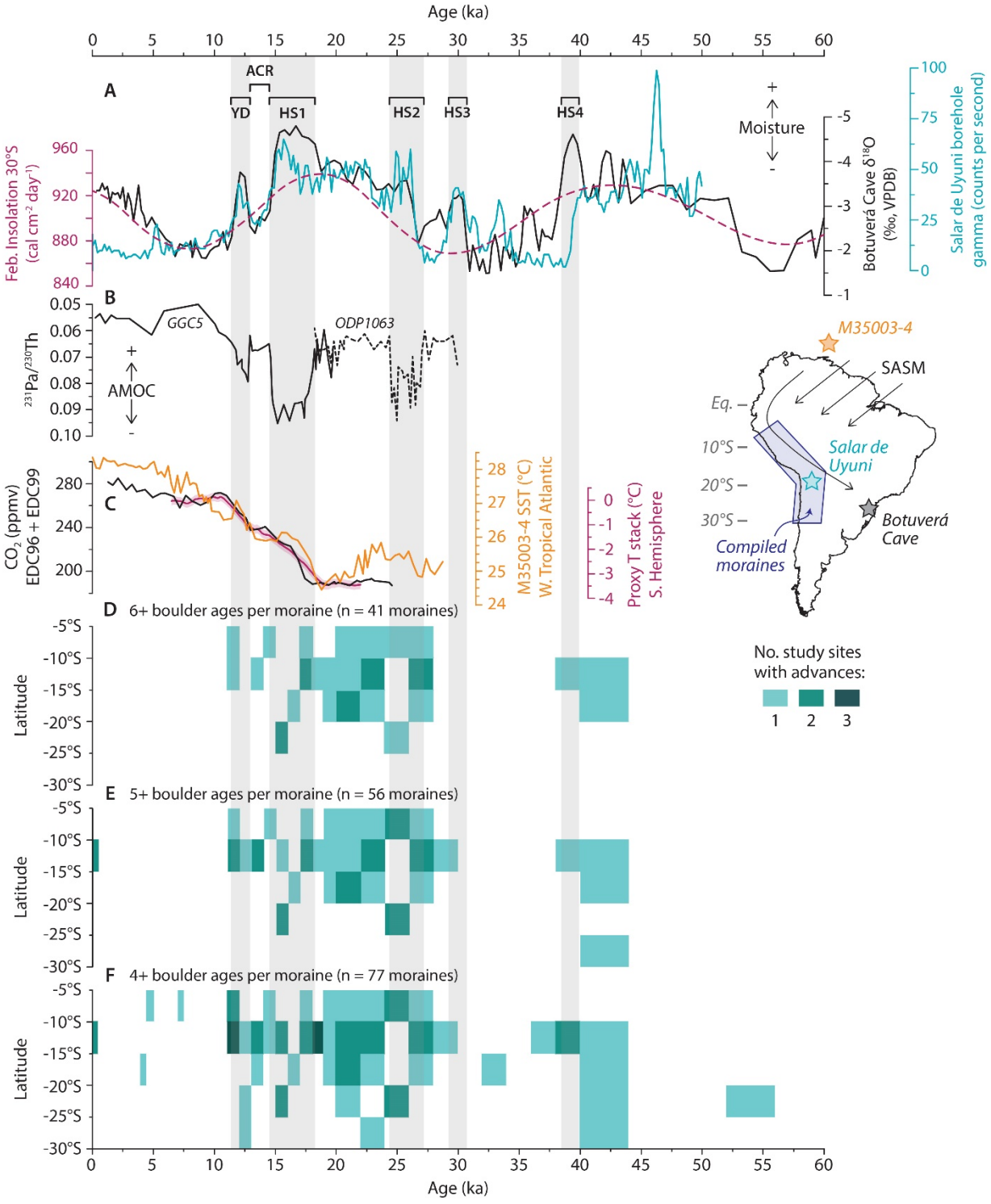


**Fig. 9. (A)** Solar insolation in February at 30°S (Berger and Loutre, 1991), the BTV-3a Botuverá Cave $\delta^{18}O$ record in southeast Brazil (Wang et al., 2007), and gamma counts from the Salar de Uyuni lake core, Bolivia (Baker at el., 2001). **(B)** The $^{231}Pa/^{230}Th$ proxy for the strength of the Atlantic Meridional Overturning Circulation (AMOC) from cores GGC5 and ODP1063 (McManus et al., 2004; Lippold et al., 2009). **(C)** Atmospheric $CO_2$ concentration reconstructed from Antarctic ice cores EDC96 and EDC99 (black; Schmitt et al., 2012), western tropical Atlantic sea surface temperatures reconstructed from core

M35003 (orange; Rühlemann et al., 1999), and a proxy stack of temperature for the Southern Hemisphere (purple; Shakun et al., 2012). **(D)** Number of dated moraines in the Central Andes that fall into 5° latitude bins and variable age bins, and have six or more clustered boulder ages each (see text for details). **(E)** The same as panel (D) but including moraines with five or more clustered boulder ages each. **(F)** The same as panel (D) but including moraines with four or more clustered boulder ages each. 'YD' = Younger Dryas; 'ACR' = Antarctic Cold Reversal; 'HS' = Heinrich Stadial.

By excluding those ages that are most likely to be unreliable, panels D-F in Fig. 9 show tighter clusters of moraine ages than the entire compilation in Fig. 6. The spatial and temporal patterns also remain similar regardless of whether the threshold number of boulder ages per moraine is set at four, five, or six. Glaciers advanced throughout the Central Andes at ~40-45 ka, during the global LGM at ~20-26 ka, and several times during the late glacial period between 11 ka and 20 ka. These broad clusters are in agreement with earlier efforts to synthesise advance timings in the region (e.g., Zech et al., 2009b). They also match the three generations of moraines we identify at the Sierra de Aconquija, showing that our results from northwestern Argentina are in agreement with the general chronology of glaciation throughout the Central Andes.

As described previously, two broad peaks in summer insolation in the Southern Hemisphere tropics/sub-tropics occurred at ~40-45 ka and ~15-25 ka, associated with an intensified SASM and wetter conditions in the Central Andes (Fig. 9a). Between 40 ka and 45 ka, glaciers advanced synchronously along more than 2000 km of the eastern margin of the Central Andes from 10°S in Peru to 27°S in Argentina. This advance coincided with the summer insolation maximum and the period of greatest depletion in the Botuverá Cave $\delta^{18}O$ record, suggesting many of these glaciers indeed responded to increased monsoonal moisture flux. Similarly, glaciers advanced across latitudes in accordance with the global LGM between 20 ka and 26-28 ka, when summer insolation increased in the southern tropics/sub-tropics, the Central Andes were relatively wet, and temperatures were low (Fig. 9a-c). These results support the interpretation that many glaciers in the Central Andes did advance in phase with intensification of the SASM during periods of increasing summer insolation in the Southern Hemisphere (e.g., Zech et al., 2008, 2009b). Additional support for this interpretation comes from the observation that, once re-interpreted, moraine ages in the Peruvian Andes exhibit ~25 ka periodicity as far back as 200-350 ka (Fig. 7).

Heinrich Stadials are recorded in the spatial pattern of moraine ages at a finer temporal resolution. The youngest (Heinrich Stadial 1, HS1; 18.0-14.7 ka) is captured in the greatest detail because of the greater precision of younger ages. Glacier advances are registered during HS1 in all latitude bins from 5°S to 25°S, starting earlier in the north and progressively

later in the south. The same spatial pattern is also observed during Heinrich Stadial 2 (HS2; 24.0-27.0 ka), although age uncertainties only permit dividing HS2 into two intervals. We infer that glaciers advanced in the Central Andes in response to increased monsoonal moisture flux during HS1 and HS2 (as well as potentially earlier Heinrich Stadials), and that the southward progression of moraine ages reflects the southward penetration of moisture during the SASM as tropical Atlantic temperatures warmed (Fig. 9d-f). This pattern in the timing of glacier advances matches the rise in sea surface temperatures and the timing of AMOC weakening (Fig. 9b-c). Furthermore, secondary peaks can be observed in both the Salar de Uyuni gamma counts and depletion of the Botuverá Cave $\delta^{18}O$ record (Fig. 9a), confirming that Heinrich Stadials were coupled with peak wet conditions at these locations. The moraine age compilation indicates that intensification of the SASM during HS1 and HS2 influenced glaciers throughout the Central Andes to a southerly limit of 25°S. The lack of moraines at the Sierra de Aconquija with ages during Heinrich Stadials (Fig. 2) supports this interpretation. As a result, the spatial distribution of moraine ages reveals sensitivity to HS1 and HS2, and shows that once unreliable records are excluded (Section 4.2), moraine ages can be used to reconstruct spatial patterns in climate variability with fine temporal and spatial resolution.

Both the ACR and YD climate events have been invoked to explain the timings of glacier advances in the Andes, but their relative importance is disputed (Bromley et al., 2011; Jomelli et al., 2014; Ward et al., 2015). Few moraines have been dated to either the YD interval or the ACR interval with 5+ boulders or 6+ boulders (i.e., the greatest confidence; Fig. 9d-e). These locations are restricted to the northern Central Andes between 5°S and 15°S, and they indicate that glaciers advanced during both events. This result matches our interpretations for the Sierra de Aconquija farther south at 27°S, where we identify both ACR and YD moraines (Fig. 8). If the threshold number of boulders per moraine is reduced to 4+ (Fig. 9f), additional sites are included in the compilation and a total of eight moraines fall between 11 ka and 13 ka (i.e., likely the YD) while five moraines fall between 13 ka and 15 ka (i.e., likely the ACR). The palaeoclimate simulation by Pedro et al. (2016) (Fig. 8b) predicts that temperatures cooled south of ~20°S and warmed north of 20°S during the ACR. Fine spatial boundaries in palaeoclimate simulations may not be entirely accurate, but it is nonetheless difficult to reconcile this simulation with multiple glacier advances during the ACR between 10°S and 20°S (Fig. 9). Further work is warranted to pinpoint exactly how far north cooling associated with the ACR penetrated in the Andes, as our compilation of moraine ages suggests this might have been ~10° farther north than modelled by Pedro et al. (2016). In contrast to the ACR, the YD was a time of weakened AMOC (Fig. 9b), a warming tropical Atlantic (Fig. 9c), intensified SASM, and increased moisture transport to the Central Andes (Fig. 9a). The results of our compilation suggest that glaciers advanced throughout the Central Andes during the YD. Our observations at the Sierra de Aconquija show that, at 27°S, the YD only resulted in minor

glaciation (see Section 5.2.3), indicating that the Sierra de Aconquija could mark the approximate southern limit of enhanced monsoonal moisture flux during the YD interval.

In summary, our re-calculation of moraine ages indicates that Central Andean glaciers advanced in response to a combination of strengthening of the South American Summer Monsoon and cool temperatures at various times during the last ~45 ka. Cross-latitude advances coincided with periods of wet climate associated with insolation maxima in the southern tropics, including during the global LGM and at ~40-45 ka. Those moraine ages likely to be most accurate indicate a ~25 ka periodicity as far back as 200-350 ka, at least in Peru (Fig. 7). The compilation of moraine ages also captures shorter-lived climate events, with advances occurring farther south in the Central Andes during Heinrich Stadials 1 and 2 and the Younger Dryas.

## 6. Conclusions

New moraine ages obtained at the Sierra de Aconquija reveal that glaciers advanced at 27°S on the eastern margin of the southern Central Andes multiple times during the last ~40 ka. We identify two large advances at approximately 22 ka and 40 ka, coincident with summer insolation maxima in the Southern Hemisphere tropics/sub-tropics. During global deglaciation, smaller advances occurred at ~13.5 ka during the Antarctic Cold Reversal and at ~12.5 ka during the Younger Dryas. One end moraine also records minor glaciation during the Bond Event 5. These results suggest that, at this location, glaciers responded sensitively to enhanced moisture delivery from the north during periods of strengthened South American Summer Monsoon, as well as to episodes of cooling in the Southern Hemisphere.

We also compiled existing $^{10}$Be data from 144 moraines in the Central Andes and re-calculated their ages using the latest age calculation parameters. To control for the accuracy of moraine age estimates at different sites, we took a uniform approach to interpreting moraine ages by selecting the oldest ages among clustered boulder exposure ages as being the closest to the timing of moraine formation. Our compilation shows that the chronology of glacier advances at the Sierra de Aconquija is in general agreement with other sites across the Central Andes. Glaciers advanced throughout the region in response to strengthening of the South American Summer Monsoon during periods of increased summer insolation in the southern tropics/sub-tropics. The compiled moraine ages also show sensitivity to millennial-scale climate events, including the Younger Dryas and Heinrich Stadials. We document a southward propagation of glacier advances during Heinrich Stadials 1 and 2, as temperatures warmed in the western tropical Atlantic and monsoonal moisture penetrated farther south in the Central Andes. Based on these data, and coupled with an absence of moraines with HS1 or HS2 ages at the Sierra

de Aconquija, we infer a southerly limit of ~25°S for enhanced monsoonal moisture flux in the Central Andes during Heinrich Stadials.

This study shows that moraine chronologies are valuable palaeoclimate indicators at local and regional scales. When a consistent analytical approach is applied, the most reliable moraine ages in the Central Andes can be used to reconstruct past climate variability at fine spatial and temporal resolutions. In addition to establishing moraine chronologies at new locations, future studies could revisit moraines dated with a small number of boulders (e.g., two or three) and supplement these with additional boulder exposure ages in order to increase the accuracy of existing chronologies. Parallel modelling efforts to invert mapped glacier extents for temperature and precipitation scenarios could exploit the growing number of dated moraines in the Central Andes to better constrain the magnitudes of past climate changes.

## 7. Acknowledgements

M. D'Arcy was supported by an Alexander von Humboldt postdoctoral fellowship, a Research Focus: Earth Sciences grant awarded by the University of Potsdam, and by the Emmy-Noether-Programm of the Deutsche Forschungsgemeinschaft (DFG) grant number SCHI 1241/1-1 awarded to T. Schildgen. M. Strecker acknowledges funds of the Deutsche Forschungsgemeinschaft provided to the IGRK StRATEGy (STR373/32-1). P. Weiss acknowledges funding by the German-Argentine university consortium (CUAA/DAHZ). We thank Miriam Dühnforth for discussions and assistance in the field. We sincerely thank Pierre-Henri Blard and an anonymous reviewer for constructive comments.

# 8. Appendix 1: Interpretation of clustered boulder ages

As outlined in Section 3, some previous studies have suggested taking the oldest boulder age within a cluster—after the exclusion of outliers attributed to nuclide inheritance—as the closest to the true timing of moraine formation (Putkonen and Swanson, 2003; Briner et al., 2005; Ivy-Ochs et al., 2007; Zech et al., 2007a,b; Applegate et al., 2010; Heyman et al., 2011; May et al., 2011; Ivy-Ochs and Briner, 2014). The reasoning behind this approach is that processes leading to incomplete exposure (e.g., differential boulder erosion, exhumation, rotation, and shielding) result in some boulder exposure ages that are younger than the moraine itself (cf. Putkonen and Swanson, 2003, Heyman et al., 2011). Here, we explore this concept further and consider how to interpret the exposure ages of boulders collected from a moraine.

## 8.1. Nuclide inheritance

Prior works identified anomalously old outliers on the grounds that they (i) sit far away from age clusters (e.g., Martini et al., 2017); (ii) violate the local stratigraphic order (e.g., Bromley et al., 2016; Ward et al., 2017; Zech et al., 2017); (iii) can be identified by statistical testing (e.g., Smith et al., 2005a,b; Jomelli et al., 2011); or (iv) by field observations that suggest a particular boulder is significantly older or was derived from hillslope debris (e.g., Martin et al., 2018). Often, these lines of evidence are used in combination and with site-specific information such as cross-cutting relationships or correlations. Collectively, these previous studies attributed 63 boulder ages to nuclide inheritance out of a total of 794, i.e., 7.9 %. This is a greater frequency than the global average of <3 % (Putkonen and Swanson, 2003), indicating that nuclide inheritance is comparatively common in the Central Andes, perhaps due to the dry climate (cf. Blard et al., 2014).We have no reason to dispute the identification of old outliers by previous studies, so we maintain the interpretation of these boulders as outliers in our compilation, and exclude them from each ‘age cluster’ associated with individual moraines.

## 8.2. Incomplete exposure

Apart from nuclide inheritance, some sampled boulders are likely to be affected by incomplete exposure effects (erosion, exhumation, toppling, and shielding) (cf. Hall et al., 2009; May et al., 2011; Shakun et al., 2015; Jomelli et al., 2014). These processes will generate exposure ages that are younger than the moraine itself, and there is evidence that these processes affect boulder exposure ages from the Central Andes. For example the dispersion of boulder ages (i.e., the difference between the oldest and youngest boulder age) on each moraine we sampled at the Sierra de Aconquija increases with moraine age (Figs 2, 5). For moraine unit

M1, we obtained clustered boulder ages between 20 ka and 40 ka, meaning that some of these ages must be incorrect. Our data compilation for the Central Andes (Fig. 4, Table 2) reveals that the dispersion of boulder ages from individual moraines increases with the oldest boulder age, such that—over four orders of magnitude in age—the data fall beneath an upper envelope where the maximum dispersion increases as about half of the oldest boulder age (Fig. A1a). Given that there is no *a priori* reason to expect older moraines to have formed over longer timescales or increasingly suffer from nuclide inheritance, this positive correlation between dispersion and age must reflect incomplete exposure bias. Boulders are more likely to have been exhumed, eroded, toppled, and shielded on older moraine surfaces. These effects are differential (variable between boulders), so the dispersion of ages increases over time as some boulders become more eroded or rotated, and an increasing number are exhumed from the moraine interior (e.g., Fig. 3d). Of course, some moraines fall below the upper envelope and can still exhibit relatively low dispersion if the sampled boulders happen to not have been shielded, or if few boulder ages were measured.

### 8.3. Boulder surface erosion

Some of the dispersion of ages is likely to be explained by erosion of the boulder surfaces (and partial loss of accumulated $^{10}$Be). We can perform a sense-check of this process by quantifying the likely magnitude of surface erosion using the boulder ages we report from the Sierra de Aconquija moraines. For each moraine, we take the youngest boulder age measured (assumed to be most affected by incomplete exposure bias) and show how its calculated age changes as a function of continuous erosion of the boulder surface (Fig. A1b, coloured lines). For example, the youngest M1 boulder has an age of 20.3 ka when calculated assuming no surface erosion (Table 3). If a correction is made for surface erosion, the exposure age increases non-linearly to ~45 ka for a surface erosion rate of 0.025 mm yr$^{-1}$. To aid comparison, the oldest boulder age obtained from each moraine (assuming zero surface erosion) is plotted as a star. If the oldest boulder age is an approximation of the true moraine age, the full dispersion of ages on each moraine could result from differential boulder surface erosion rates that range between zero (producing the oldest age in the cluster) and the maximum erosion rate indicated by the star (producing the youngest age in the cluster).

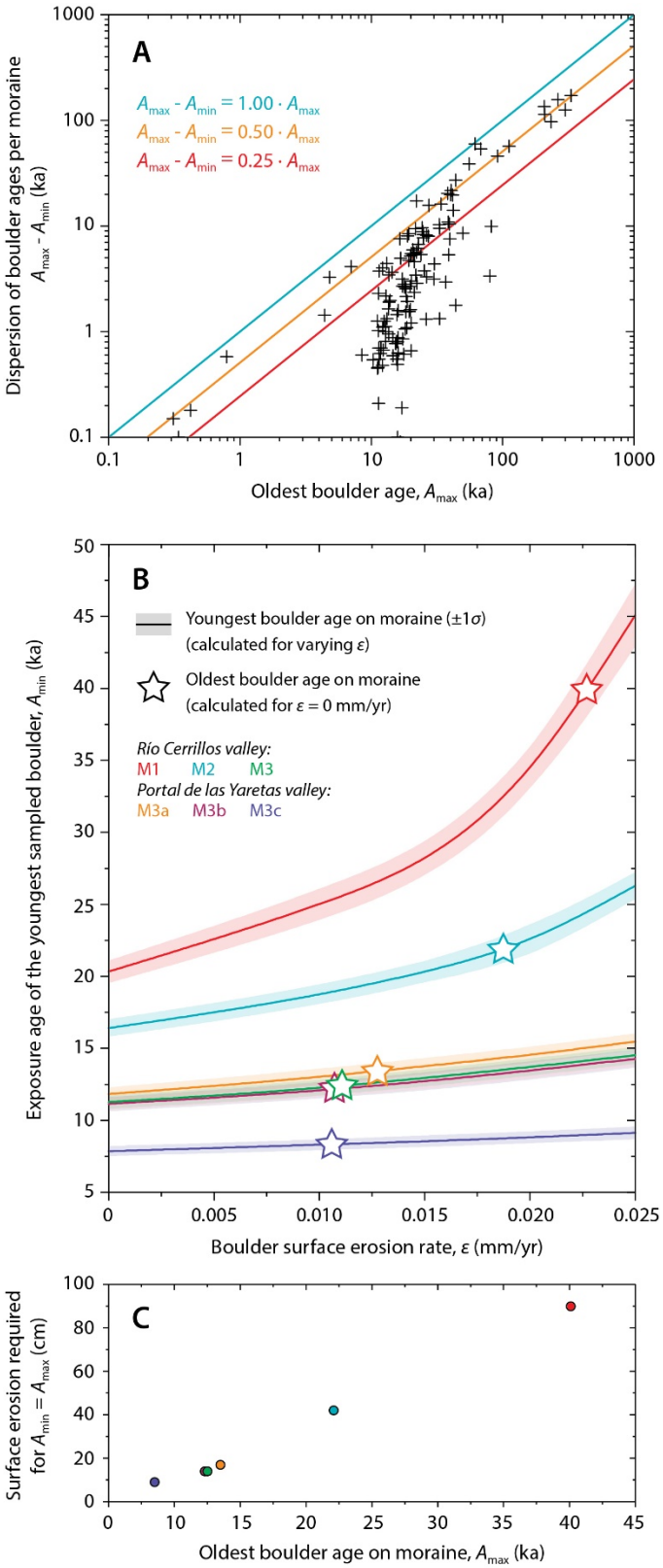


**Fig. A1. (A)** The dispersion of boulder ages for each moraine compiled in the Central Andes (i.e., the oldest boulder age, $A_{max}$, minus the youngest boulder age, $A_{min}$) plotted against the oldest boulder age. Both axes are logged. Old outliers due to inheritance were first eliminated in keeping with the original studies. The data fall below an upper envelope for which the dispersion increases as approximately half of the oldest boulder age. **(B)** The estimated age of the *youngest* boulder sampled on each moraine unit ($A_{min}$) at the Sierra de Aconquija, as a function of the assumed boulder surface erosion rate, $\varepsilon$. For faster assumed boulder surface erosion rates, the erosion-corrected exposure age is greater. Coloured shading indicates ±1σ uncertainty. Stars show the ages of the *oldest* boulder sampled on the moraine for comparison (following exclusion of clear outliers affected by inheritance), which likely approximates the age of moraine deposition (see text). Overall, the youngest age ($A_{min}$) from the older moraine units require a higher erosion rates to match to the oldest age ($A_{max}$) from the same unit. **(C)** The total amount of boulder surface erosion required to increase the value of $A_{min}$ to make it equal to $A_{max}$ (assuming no erosion for $A_{max}$). This is the maximum amount of differential boulder erosion needed on each moraine unit to explain the full dispersion of boulder ages entirely as a function of erosion.

For the M3 moraines, the youngest boulder ages would increase to match the oldest boulder age in each cluster (i.e., the dispersion would be completely eliminated) with erosion rates of

~0.01 mm $yr^{-1}$ (Fig. A1b). Over the full exposure history of the boulders, this is equivalent to losing 10-20 cm of material from the boulder surfaces (Fig. A1c). This thickness is a maximum estimate firstly because it is calculated for the youngest boulder on each moraine, and secondly because it does not invoke any other processes such as toppling or shielding. The loss of a few centimetres from the boulder surface over a period of 10-15 ka is a realistic scenario, and may be impossible to identify when sampling in the field. For the older M2 and M1 moraines, the erosion rate required to reconcile the youngest and oldest ages in each cluster increase to ~0.019 and ~0.023 mm $yr^{-1}$, respectively. This is equivalent to removing 40 cm and 90 cm of material from the tops of individual boulders over timespans of 20 ka and 40 ka, respectively. We interpret these amounts to be less realistic based on our field observations; as a result, additional processes (boulder exhumation, toppling, and shielding) must be invoked for the older moraines to explain the age dispersion. This result is expected, as older moraines will have experienced more topographic decay, and therefore more boulder exhumation and disturbance. Our analyses of the dispersion-age pattern and maximum boulder erosion rates thus supports previous studies (Putkonen and Swanson, 2003; Briner et al., 2005; Heyman et al., 2011; Ivy-Ochs and Briner, 2014) that recommend taking the oldest boulder age within an age cluster (after the elimination of outliers due to nuclide inheritance) to be the closest to the true moraine age.

### 8.4. Alternative approaches

For the reasons outlined above, we take the oldest clustered boulder age, after the elimination of outliers attributed to nuclide inheritance, as closest to the actual moraine age. This approach recognises that boulder ages collected from moraines can be too old (due to nuclide inheritance) or too young (due to erosion, exhumation, toppling, and shielding processes), and has been taken by numerous prior studies in the Central Andes (Zech et al., 2006, 2007a,b, 2009b, 2010; 2017; Hall et al., 2009; May et al., 2011). However, alternative approaches are also taken and there is currently no consensus about how to best interpret a moraine age from a spread of boulder ages. Some studies choose to only eliminate old outliers attributed to nuclide inheritance, and then average all remaining boulder ages, for example using a frequency density plot (Smith and Rodbell, 2010; Jomelli et al., 2011; Smith et al., 2011; Ward et al., 2015; Martin et al., 2018) or a mean value (Licciardi et al., 2009; Shakun et al., 2015b; Stansell et al., 2015, 2017; Bromley et al., 2016; Martini et al., 2017). It is therefore important to address whether these alternative approaches would result in significantly different moraine chronologies and palaeoclimatic interpretations. We explore this possibilitiy in Fig. A2.

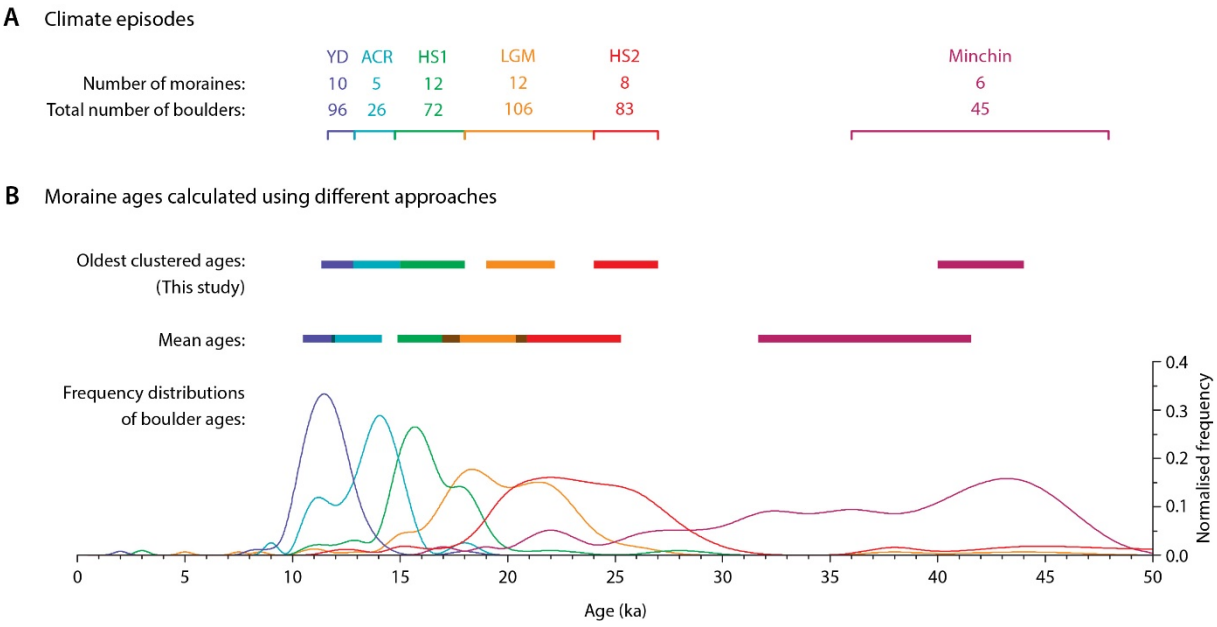


**Fig. A2.** Comparison of moraine ages calculated using different approaches. **(A)** Moraines in the Central Andes (from the compilation in this study) with 4 or more clustered boulder ages were grouped according to which climatic episode they coincide with, as interpreted in this study. **(B)** The range of moraine ages in each group, calculated using different approaches. The oldest clustered boulder age approach (used in this study, top row) and mean ages (bottom row) are shown with coloured bars; in both cases all boulder ages interpreted by the original studies to be outliers resulting from nuclide inheritance were first excluded. Frequency distributions are shown below. For each climatic episode, all boulder ages from all moraines (including outliers attributed to nuclide inheritance) are plotted as a single frequency distribution normalised to a sum of 1. As these distributions incorporate a statistically meaningful sample size of boulders from moraines of equivalent age (between 26-106 boulders per curve), their shapes are significant.

To perform this comparison of approaches to determining moraine ages, we selected all moraines in our compilation that have 4 or more boulder ages (see section 4.2) and have been interpreted to coincide with specific climate episodes. We chose the Younger Dryas, the Antarctic Cold Reversal, Heinrich Stadials 1 and 2, the global LGM, and the Minchin pluvial episode because these episodes include a significant number of well-sampled moraines of equivalent age. For each climate episode (indicated with colours), the range of individual moraine ages are shown when calculated using three different approaches: (i) the oldest clustered boulder age approach that we favour in this study; (ii) mean values of boulder ages; and (iii) frequency distributions of boulder ages. For the oldest clustered/mean ages we first excluded boulder ages attributed to nuclide inheritance by the original studies. The frequency distributions include all boulder ages, as their shapes may reveal information about the relative

importance of old and young outliers. Pooling data from multiple moraines in this way is essential for interpreting the shapes of the resulting frequency distributions, which require a significant number of data points to be meaningful.

There is relatively close agreement between the moraine ages whether they are derived using the 'oldest clustered boulder age' approach, the mean values of clustered boulder ages, or the peaks of boulder age frequency distributions. The latter two approaches naturally result in slightly younger moraine ages because they include the youngest boulder ages obtained on each moraine. This discrepancy—the shift towards slightly younger ages for the mean age and frequency distribution approaches compared to the oldest clustered age approach—increases in magnitude as a function of moraine age. This observation is critical, because it presumably reflects the increasing importance of processes like boulder erosion, exhumation, rotation, and shielding in affecting boulder exposure ages as moraines become older. Furthermore, the frequency distributions in Fig. A2b are generally symmetrical, implying that both nuclide inheritance and incomplete exposure biases are present and should be addressed. For the older "Michin" moraines, the distribution has a negative skew (a longer 'young tail'), which indicates that processes like boulder erosion and moraine degradation become more important as moraines age.

For the reasons outlined in this Appendix, we favour the selection of the oldest clustered boulder age, after outliers attributed to nuclide inheritance have been excluded, as closest to the timing of glacier advance (in agreement with Putkonen and Swanson, 2003; Briner et al., 2005; Ivy-Ochs et al., 2007; Zech et al., 2007a,b; Applegate et al., 2010; Heyman et al., 2011; May et al., 2011; Ivy-Ochs and Briner, 2014). Prior studies have identified that nuclide inheritance is a significant issue for Central Andean moraines. We maintain this interpretation: in defining the cluster of boulder ages for each moraine, we exclude all outliers affected by inheritance that were indentified by the original studies. Equally, we accept that many boulders are also affected by erosion, exhumation, toppling, and shielding, which may be impossible to identify when sampling boulders in the field. Evidence in support of the importance of these processes includes (i) the dispersion-age relationship in Fig. A1a; (ii) our sense-check calculations of boulder surface erosion in Fig. A1b-c; (iii) the increasing discrepancy over time between moraine ages derived using the oldest clustered age approach versus approaches that do not account for incomplete exposure; (iv) the shapes of boulder age frequency distributions that collate statistically meaningful sample sizes (Fig. A2b); and (v) field observations (Fig. 3). Nevertheless, Fig. A2b reveals that taking alternative approaches to interpreting moraine ages (i.e., identifying peaks in frequency distributions or calculating means of clustered boulder ages) would not change the fundamental palaeoclimate interpretations of this study, especially for moraines dating to the last ~30 ka. There is

significant overlap between moraine ages calculated using the different approaches, and the same relative age order of advances, with discrepancies of only 1-2 ka for LGM moraines and younger.

## 9. References


Ahumada, A.,L., Páez, G.P., Ibáñez Palacios, G.P. (2013) Los glaciares de escombros en la sierra de Aconquija, Argentina. Acta geológica lilloana, **25**, 49-68.

Alley, R.B., Mayewski, P.A., Sowers, T., Stuiver, M., Taylor, K.C., Clark, P.U. (1997) Holocene climatic instability: A prominent, widespread event 8200 yr ago. *Geology*, **25**, 483-486.

Applegate, P.J., Urban, N.M., Laabs, B.J.C., Alley, R.B. (2010) Modeling the statistical distributions of cosmogenic nuclide exposure dates from moraines. *Geoscientific Model Development*, **3**, 292-307.

Baker, P.A., Fritz, S.C. (2015) Nature and causes of Quaternary climate variation of tropical South America. *Quaternary Science Reviews*, **124**, 31-47.

Baker, P.A., Rigsby, C.A., Seltzer, G.O., Fritz, S.C., Lowenstein, T.K., Bacher, N.P., Veliz, C. (2001) Tropical Climate Changes at Millennial and Orbital Timescales on the Bolivian Altiplano. *Nature*, **409**, 698-701.

Balco G, Stone JO, Lifton NA and Dunai TJ. (2008) A complete and easily accessible means of calculating surface exposure ages or erosion rates from $^{10}$Be and $^{26}$Al measurements. *Quaternary Geochronology*, **3**, 174-195.

Barber, D.C., Dyke, A., Hillaire-Marcel, C., Jennings, A.E., Andrews, J.T., Kerwin, M.W., Bilodeau, G., McNeely, R., Southon, J., Morehead, M.D., Gagnon, J.-M. (1999) Forcing of the cold event of 8,200 years ago by catastrophic drainage of Laurentide lakes. *Nature*, **400**, 344-348.

Bekaddour, T., Schlunegger, F., Vogel, H., Delunel, R., Norton, K.P., Akçar, N., Kubik, P. (2014) Paleo erosion rates and climate shifts recorded by Quaternary cut-and-fill sequences in the Pisco valley, central Peru. *Earth and Planetary Science Letters*, **390**, 103-115.

Berger, A., Loutre, M.F. (1991) Insolation values for the climate of the last 10 million years. *Quaternary Science Reviews*, **10**, 297-317.

Bianchi, A.R., Yañez, C.E. (Eds) (1992) Las Precipitaciones en el Noroeste Argentino. Instituto Nacional de Tecnologia Agropecuaria, Estacion Experimental Agropecuaria, Salta, pp. 393.

Blard, P.-H., Braucher, R., Lavé, J., Bourlès, D. (2013) Cosmogenic $^{10}$Be production rate calibrated against $^{3}$He in the high Tropical Andes (3800-4900 m, 20-22° S). *Earth and Planetary Science Letters*, **382**, 140-149.

Blard, P.-H., Lavé, J., Farley, K.A., Fornari, M., Jiménez, N., Ramirez, V. (2009) Late local glacial maximum in the Central Altiplano triggered by cold and locally-wet conditions during the paleolake Tauca episode (17-15 ka, Heinrich 1). *Quaternary Science Reviews*, **28**, 3414-3427.

Blard, P.-H., Lavé, J., Farley, K.A., Ramirez, V., Jimenez, N., Martin, L.C.P., Charreau, J., Tibari, B., Fornari, M. (2014) Progressive glacial retreat in the Southern Altiplano (Uturuncu volcano, 22°S) between 65 and 14 ka constrained by cosmogenic $^{3}$He dating. *Quaternary Research*, **82**, 209-221.

Blard, P.-H., Sylvestre, F., Tripati, A.K., Claude, C., Causse, C., Coudrain, A., Condom, T., Seidel, J.-L., Vimeux, F., Moreau, C., Dumoulin, J.-P., Lavé, J. (2011). Lake highstands on the Altiplano (Tropical

Andes) contemporaneous with Heinrich 1 and the Younger Dryas: new insights from $^{14}C$, U-Th dating and $\delta^{18}O$ of carbonates *Quaternary Science Reviews*, **30**, 3973-3989.

Blunier, T., Schwander, J., Stauffer, B., Stocker, T., Dällenbach, A., Indermühle, A., Tschumi, J., Chappellaz, J., Raynaud, D., Barnola, J.-M. (1997) Timing of the Antarctic Cold Reversal and the atmospheric $CO_2$ increase with respect to the Younger Dryas event. *Geophysical Research Letters*, **24**, 2683-2686.

Bobst, A.L., Lowenstein, T.K., Jordan, T.E., Godfrey, L.V., Ku, T.-L., Luo, S. (2001) A 106 ka paleoclimate record from drill core of the Salar de Atacama, northern Chile. *Palaeogeography, Palaeoclimatology, Palaeoecology*, **173**, 21-42.

Bond, G., Showers, W., Cheseby, M., Lotti, R., Almasi, P., deMenocal, P., Priore, P., Cullen, H., Hajdas, I., Bonani, G. (1997) A pervasive millennial-scale cycle in North Atlantic Holocene and glacial climates. *Science*, **278**, 1257-1266.

Bookhagen, B., Haselton, K., Trauth, M.H. (2001) Hydrological modelling of a Pleistocene landslide-dammed lake in the Santa Maria Basin, NW Argentina. *Palaeogeography, Palaeoclimatology, Palaeoecology*, **169**, 113-127.

Bookhagen, B., Strecker, M.R. (2008) Orographic barriers, high-resolution TRMM rainfall, and relief variations along the eastern Andes. *Geophysical Research Letters*, **35**, L06403.

Briner, J.P., Kaufman, D.S., Manley, W.F., Finkel, R.C., Caffee, M.W. (2005) Cosmogenic exposure dating of late Pleistocene moraine stabilization in Alaska. *Geological Society of America Bulletin*, **117**, 1108-1120.

Bromley, G.R.M., Hall, B.L., Rademaker, K.M., Todd, C.E., Racovteanu, A.E. (2011) Late Pleistocene snowline fluctuations at Nevado Coropuna (15°S), southern Peruvian Andes. *Journal of Quaternary Science*, **26**, 305-317.

Bromley, G.R.M., Schaefer, J.M., Hall, B.L., Rademaker, K.M., Putnam, A.E., Todd, C.E., Hegland, M., Winckler, G., Jackson, M.S., Strand, P.D. (2016) A cosmogenic $^{10}Be$ chronology for the local last glacial maximum and termination in the Cordillera Oriental, southern Peruvian Andes: Implications for the tropical role in global climate. *Quaternary Science Reviews*, **148**, 54-67.

Bromley, G.R.M., Schaefer, J.M., Winckler, G., Hall, B.L., Todd, C.E., Rademaker, K.M. (2009) Relative timing of last glacial maximum and late-glacial events in the central tropical Andes. *Quaternary Science Reviews*, **28**, 2514-2526.

Castino, F., Bookhagen, B., Strecker, M.R. (2016) Rainfall variability and trends of the past six decades (1950–2014) in the subtropical NW Argentine Andes. *Climate Dynamics*, **48**, 1049-1067.

Cheng, H., Sinha, A., Cruz, F.W., Wang, X., Edwards, R.L., d'Horta, F.M., Ribas, C.C., Vuille, M., Stott, L.D., Auler, A.S. (2013) Climate change patterns in Amazonia and biodiversity. *Nature Communications*, **4**, 1411.

Chepstow-Lusty, A., Bush, M.B., Frogley, M.R., Baker, P.A., Fritz, S.C., Aronso, J. (2005) Vegetation and climate change on the Bolivian Altiplano between 108,000 and 18,000 yr ago. *Quaternary Research*, **63**, 90-98.

Chiang, J.C.H., Biasutti, M., Battisti, D.S. (2003) Sensitivity of the Atlantic Intertropical Convergence Zone to Last Glacial Maximum boundary conditions. *Paleoceanography*, **18**, 1094.

Clapperton, C.M., Clayton, J.D., Benn, D.I., Marden, C.J., Argollo, J. (1997) Late Quaternary glacier advances and palaeolake highstands in the Bolivian Altiplano. *Quaternary International*, **38/39**, 49-59.

Cook, K.H., Vizy, E.K. (2006) South American climate during the Last Glacial Maximum: Delayed onset of the South American monsoon. *Journal of Geophysical Research*, **111**, D02110.

Crivellari, S., Chiessi, C.M., Kuhnert, H., Häggi, C., Portilho-Ramos, R.C., Zeng, J.-Y., Zhang, Y., Schefuβ, E., Mollenhauer, G., Hefter, J., Alexandre, F., Sampaio, G., Mulitza, S. (2018) Increased Amazon freshwater discharge during late Heinrich Stadial 1. *Quaternary Science Reviews*, **181**, 144-155.

Cruz, F.W., Jr., Burns, S.J., Karmann, I., Sharp, W.D., Vuille, M., Cardoso, A.O., Ferrari, J.A., Silva Dias, P.L., Viana, O., Jr. (2005) Insolation-driven changes in atmospheric circulation over the past 116,000 years in subtropical Brazil. *Nature*, **434**, 63-66.

Farber, D.L., Hancock, G.S., Finkel, R.C., Rodbell, D.C. (2005) The age and extent of tropical alpine glaciation in the Cordillera Blanca, Peru. *Journal of Quaternary Science*, **20**, 759-776.

Fornace, K., Shanahan, T.M., Sylva, S., Ossolinski, J., Baker, P.A., Fritz, S.C., Hughen, K., 2011. Hydrologic and temperature variability at Lake Titicaca over the past 50,000 years. In: AGU Fall Meeting, San Francisco.

Fornace, K.L., Whitney, B.S., Galy, V., Hughen, K.A., Mayle, F.E. (2016) Late Quaternary environmental change in the interior South American tropics: new insight from leaf wax stable isotopes. *Earth and Planetary Science Letters*, **438**, 75-85.

Fritz, S.C., Baker, P.A., Seltzer, G.O., Ballantyne, A., Tapia, P., Cheng, H., Edwards, R.L. (2007) Quaternary glaciation and hydrologic variation in the South American tropics as reconstructed from the Lake Titicaca drilling project. *Quaternary Research*, **68**, 410-420.

Garreaud, R.D., Vuille, M., Compagnucci, R., Marengo, J. (2003) Present-day South American climate. *Palaeogeography, Palaeoclimatology, Palaeoecology*, **281**, 180-195.

Glasser, N.F., Clemmens, S., Schnabel, C., Fenton, C.R., McHargue, L. (2009) Tropical glacier fluctuations in the Cordillera Blanca, Peru between 12.5 and 7.6 ka from cosmogenic $^{10}$Be dating. *Quaternary Science Reviews*, **28**, 3448-3458.

Hall, S.R., Farber, D.L., Ramage, J.M., Rodbell, D.T., Finkel, R.C., Smith, J.A., Mark, B.G., Kassel, C. (2009) Geochronology of Quaternary glaciations from the tropical Cordillera Huayhuash, Peru. *Quaternary Science Reviews*, **28**, 2991-3009.

Haselton, K., Hilley, G., Strecker, M.R. (2002) Average Pleistocene climatic patterns in the Southern Central Andes: Controls on mountain glaciation and palaeoclimate implications. *Journal of Geology*, **110**, 211-226.

Haug, G.H., Hughen, K.A., Sigman, D.M., Peterson, L.C., Röhl, U. (2001) Southward migration of the Intertropical Convergence Zone through the Holocene. *Science*, **293**, 1304-1308.

He, F., Shakun, J.D., Clark, P.U., Carlson, A.E., Liu, Z., Otto-Bliesner, B., Kutzbach, J.E. (2013) Northern Hemisphere forcing of Southern Hemisphere climate during the last deglaciation. *Nature*, **494**, 81-85.

Heyman, J., Stroeven, A.P., Harbor, J.M., Caffee, M.W. (2011) Too young or too old: Evaluating cosmogenic nuclide exposure dating based on an analysis of compiled boulder ages. *Earth and Planetary Science Letters*, **302**, 71-80.

Heyman, J., Applegate, P.J., Blomdin, R., Gribenski, N., Harbor, J.M., Stroeven, A.P. (2016) Boulder height-exposure age relationships from a global glacial $^{10}$Be compilation. *Quaternary Geochronology*, **34**, 1-11.

Hillyer, R., Valencia, B.G., Bush, M.B., Silman, M.R., Steinitz-Kannan, M. (2009) A 24,700-yr paleolimnological history from the Peruvian Andes. *Quaternary Research*, **71**, 71-82.

Ivy-Ochs, S., Briner, J.P. (2014) Dating disappearing ice with cosmogenic nuclides. *Elements*, **10**, 351-356.

Ivy-Ochs, S., Kerschner, H., Schlüchter, C. (2007) Cosmogenic nuclides and the dating of Lateglacial and Early Holocene glacier variations: The Alpine perspective. *Quaternary International*, **164-165**, 53-63.

Jomelli, V., Favier, V., Vuille, M., Braucher, R., Martin, L., Blard, P.-H., Colose, C., Brunstein, D., He, F., Khodri, M., Bourlès, D.L., Leanni, L., Rinterknecht, V., Grancher, D., Francou, B., Ceballos, J.L., Fonseca, H., Liu, Z., Otto-Bliesner, B.L. (2014) A major advance of tropical Andean glaciers during the Antarctic cold reversal. *Nature*, **513**, 224-228.

Jomelli, V., Khodri, M., Favier, V., Brunstein, D., Ledru, M.-P., Wagnon, P., Blard, P.-H., Sicart, J.-E., Braucher, R., Grancher, D., Bourlès, D.L., Braconnot, P., Vuille, M. (2011) Irregular tropical glacier retreat over the Holocene epoch driven by progressive warming. *Nature*, **474**, 196-199.

Jomelli, V., Martin, L., Blard, P.-H., Favier, V., Vuille, M., Ceballos, J.L. (2017) Revisiting the Andean tropical glacier behaviour during the Antarctic Cold Reversal. *Geographical Research Letters*, **43**, 629-648.

Kanner, L.C., Burns, S.J., Cheng, H., Edwards, R.L. (2012) High-Latitude Forcing of the South American Summer Monsoon During the Last Glacial. *Science*, **335**, 570-573.

Kelly, M.A., Lowell, T.V., Applegate, P.J., Phillips, F.M., Schaefer, J.M., Smith, C.A., Kim, H., Leonard, K.C., Hudson, A.M. (2015) A locally calibrated, late glacial $^{10}$Be production rate from a low-latitude, high-altitude site in the Peruvian Andes. *Quaternary Geochronology*, **26**, 70-85.

Kelly, M.A., Lowell, T.V., Applegate, P.J., Smith, C.A., Phillips, F.M., Hudson, A.M. (2012) Late glacial fluctuations of Quelccaya Ice Cap, southeastern Peru. *Geology*, **40**, 991-994.

Kirkbride, M.P., Winkler, S. (2012) Correlation of Late Quaternary moraines: Impact of climate variability, glacier response, and chronological resolution. *Quaternary Science Reviews*, **46**, 1-29.

Kohl, C.P., Nishiizumi, K. (1992) Chemical isolation of quartz for measurement of in-situ-produced cosmogenic nuclides. *Geochimica et Cosmochimica Acta*, **56**, 3583-3587.

Kull, C., Imhof, S., Grosjean, M., Zech, R., Veit, H. (2008) Late Pleistocene glaciation in the Central Andes: Temperature versus humidity control — A case study from the eastern Bolivian Andes (17°S) and regional synthesis. *Global and Planetary Change*, **60**, 148-164.

Lal, D. (1991) Cosmic ray labeling of erosion surfaces: In situ nuclide production rates and erosion models. *Earth and Planetary Science Letters*, **104**, 424-439.

Licciardi, J.M., Schaefer, J.M., Taggart, J.R., Lund, D.C. (2009) Holocene Glacier Fluctuations in the Peruvian Andes Indicate Northern Climate Linkages. *Science*, **325**, 1677-1679.

Lippold, J., Gruetzner, J., Winter, D., Lahaye, Y., Mangini, A., Christl, M. (2009) Does sedimentary $^{231}$Pa/$^{230}$Th from the Bermuda Rise monitor past Atlantic Meridional Overturning Circulation? *Geophysical Research Letters*, **36**, L12601.

Liu, Z., Otto-Bliesner, B.L., He, F., Brady, E.C., Tomas, R., Clark, P.U., Carlson, A.E., Lynch-Stieglitz, J., Curry, W., Brook, E., Erickson, D., Jacob, R., Kutzbach, J., Cheng, J. (2009) Transient simulation of last deglaciation with a new mechanism for Bølling-Allerød warming. *Science*, **325**, 310-314.

Luna, L.V., Bookhagen, B., Niedermann, S., Rugel, G., Scharf, A., Merchel, S. (2018) Glacial chronology and production rate cross-calibration of five cosmogenic nuclide and mineral systems from the southern Central Andean Plateau. *Earth and Planetary Science Letters*, **500**, 242-253.

Maldonado A, Betancourt JL, Latorre C, Villagran C. (2005) Pollen analyses from a 50,000-yr rodent midden series in the southern Atacama Desert (25°30 S). *Journal of Quaternary Science*, **20**, 493–507.

Marengo, J.A., Liebmann, B., Grimm, A.M., Misra, V., Silva Dias, P.L., Cavalcanti, I.F.A., Carvalho, L.M.V., Berbery, E.H., Ambrizzi, T., Vera, C.S., Saulo, A.C., Nogues-Paegle, J., Zipser, E., Seth, A.,

Alves, A.M. (2010) Recent developments on the South American monsoon system. *International Journal of Climatology*, **32**, 1-21.

Marrero, S.M., Phillips, F.M., Borchers, B., Lifton, N., Aumer, R., Balco, G. (2016) Cosmogenic nuclide systematics and the CRONUScalc program. *Quaternary Geochronology*, **31**, 160-187.

Martin, L.C.P., Blard, P.-H., Balco, G., Lavé, J., Delunel, R., Lifton, N., Laurent, V. (2017) The CREp program and the ICE-D production rate calibration database: A fully parameterizable and updated online tool to compute cosmic-ray exposure ages. *Quaternary Geochronology*, **38**, 25-49.

Martin, L.C.P., Blard, P.-H., Lavé, J., Braucher, R., Lupker, M., Condom, T., Charreau, J., Mariotti, V., ASTER Team, Davy, E. (2015) In situ cosmogenic $^{10}$Be production rate in the High Tropical Andes. *Quaternary Geochronology*, **30**, 54-68.

Martin, L.C.P., Blard, P.-H., Lavé, J., Condom, T., Prémaillon, M., Jomelli, V., Brunstein, D., Lupker, M., Charreau, J., Mariotti, V., Tibari, B., ASTER Team, Davy, E. (2018) Lake Tauca highstand (Heinrich Stadial 1a) driven by a southward shift of the Bolivian High. *Science Advances*, **4**, eaar2514.

Martini, M.A., Kaplan, M.R., Strelin, J.A., Astini, R.A., Schaefer, J.M., Caffee, M.W., Schwartz, R. (2017) Late Pleistocene glacial fluctuations in Cordillera Oriental, subtropical Andes. *Quaternary Science Reviews*, **171**, 245-259.

May, J.-H., Zech, J., Zech, R., Preusser, F., Argollo, J., Kubik, P.W., Veit, H. (2011) Reconstruction of a complex late Quaternary glacial landscape in the Cordillera de Cochabamba (Bolivia) based on a morphostratigraphic and multiple dating approach. *Quaternary Research*, **76**, 106-118.

McManus, J.F., Francois, R., Gherardi, J.-M., Keigwin, L.D., Brown-Leger, S. (2004) Collapse and rapid resumption of Atlantic meridional circulation linked to deglacial climate changes. *Nature*, **428**, 834–837.

Montade, V., Kageyama, M., Combourieu-Nebout, N., Ledru, M.-P., Michel, E., Siani, G., Kissel, C. (2015) Teleconnection between the Intertropical Convergence Zone and southern westerly winds throughout the last deglaciation. *Geology*, **43**, 735-738.

Moreiras, S.M., Páez, M.S., Lauro, C., Jeanneret, P. (2017) First cosmogenic ages for glacial deposits from the Plata range (33°S): New inferences for Quaternary landscape evolution in the Central Andes. *Quaternary International*, **438**, 50-64.

Moreno, P.I., Kaplan, M.R., François, J.P., Villa-Martínez, R., Moy, C.M., Stern, C.R., Kubik, P.W. (2009) Renewed glacial activity during the Antarctic Cold Reversal and persistence of cold conditions until 11.5 ka in SW Patagonia. *Geology*, **37**, 375-378.

Mosblech, N.A.S., Bush, M.B., Gosling, W.D., Hodell, D., Thomas, L., van Calsteren, P., Correa-Metrio, A., Valencia, B.G., Curtis, J., van Woesik, R. (2012) North Atlantic forcing of Amazonian precipitation during the last ice age. *Nature Geoscience*, **5**, 817-820.

Muscheler, R., Beer, J., Kubik, P.W., Synal, H.-A. (2005) Geomagnetic field intensity during the last 60,000 years based on $^{10}$Be and $^{36}$Cl from the Summit ice cores and $^{14}$C. *Quaternary Science Reviews*, **24**, 1849-1860.

National Oceanic and Atmospheric Administration, NOAA (1976) U.S. Standard Atmosphere. US Government Printing Office.

Nester, P.L., Gayó, E., Latorre, C., Jordan, T.E., Blanco, N. (2007) Perennial stream discharge in the hyperarid Atacama Desert of northern Chile during the latest Pleistocene. *Proceedings of the National Academy of Sciences*, **104**, 19,724-19,729.

Nishiizumi, K., Imamura, M., Caffee, M.W., Southon, J.R., Finkel, R.C., McAninch, J. (2007) Absolute calibration of $^{10}$Be AMS standards. *Nuclear Instruments and Methods in Physics Research Section B: Beam Interactions with Materials and Atoms*, **258**, 403-413.

North Greenland Ice Core Project Members (2004) High-resolution record of Northern Hemisphere climate extending into the last interglacial period. *Nature*, **431**, 147-151.

Novello, V.F., Cruz, F.W., Vuille, M., Stríkis, N.M., Edwards, R.L., Cheng, H., Emercik, S., de Paula, M.S., Li, X., Barreto, E.S., Karmann, I., Santos, R.V. (2017) A high-resolution history of the South American Monsoon from Last Glacial Maximum to the Holocene. *Scientific Reports*, **7**, 44267.

Pedro, J.B., Bostock, H.C., Bitz, C.M., He, F., Vandergoes, M.J., Steig, E.J., Chase, B.M., Krause, C.E., Rasmussen, S.O., Markle, B.R., Cortese, G. (2016) The spatial extent and dynamics of the Antarctic Cold Reversal. *Nature Geoscience*, **9**, 51-55.

Pedro, J.B., van Ommen, T.D., Rasmussen, S.O., Morgan, V.I., Chappellaz, J., Moy, A.D., Masson-Delmotte, V., Delmotte, M. (2011) The last deglaciation: timing the bipolar seesaw. *Climate of the Past*, **7**, 671-683.

Peterson, L.C., Haug, G.H., Hughen, K.A., Röhl, U. (2000) Rapid Changes in the Hydrologic Cycle of the Tropical Atlantic During the Last Glacial. *Science*, **290**, 1947-1951.

Placzek, C., Quade, J., Patchett, P.J. (2006) Geochronology and stratigraphy of late Pleistocene lake cycles on the southern Bolivian Altiplano: Implications for causes of tropical climate change. *Geological Society of America Bulletin*, **118**, 515-532.

Placzek, C.J., Quade, J., Patchett, P.J. (2013) A 130 ka reconstruction of rainfall on the Bolivian Altiplano. *Earth and Planetary Science Letters*, **363**, 97-108.

Portilho-Ramos, R.C., Chiessi, C.M., Zhang, Y., Multiza, S., Kucera, M., Siccha, M., Prange, M., Paul, A. (2017) Coupling of equatorial Atlantic surface stratification to glacial shifts in the tropical rainbelt. *Scientific Reports*, **7**, 1561.

Prohaska, F. (1976) The climate of Argentina, Paraguay and Uruguay. In: Climates of Central and South America. In: World Survey of Climatology. Vol. 12, Schwerdtfeger, W. (Ed.), Elsevier, Amsterdam, 13-73.

Putkonen, J., Swanson, T. (2003) Accuracy of cosmogenic ages for moraines. *Quaternary Research*, **59**, 255-261.

Putnam, A.E., Denton, G.H., Schaefer, J.M., Barrell, D.J.A., Anderson, B.G., Finkel, R.C., Schwartz, R., Doughty, A.M., Kaplan, M.R. (2010) Glacier advance in southern middle-latitudes during the Antarctic Cold Reversal. *Nature Geoscience*, **3**, 700-704.

Ramirez, E., Hoffmann, G., Taupin, J.D., Francou, B., Ribstein, P., Caillon, N., Ferron, F.A., Landais, A., Petit, J.R., Pouyaud, B., Schotterer, U., Simoes, J.C., Stievenard, M. (2003) A new Andean deep ice core from Nevado Illimani (6350 m), Bolivia. *Earth and Planetary Science Letters*, **212**, 337-350.

Rodbell, D.T., Smith, J.A., Mark, B.G. (2009) Glaciation in the Andes during the Lateglacial and Holocene. *Quaternary Science Reviews*, **28**, 2165-2212.

Rohling, E.J., Pälike, H. (2005) Centennial-scale climate cooling with a sudden cold event around 8,200 years ago. *Nature*, **434**, 975-979.

Rohmeder, W. (1941) Die diluviale Vereisung des Aconquija-Gebirges in Nordwest-Argentinien. *Petermann. Geogr. Mitt.,* **12**, 417-433.

Rühlemann, C., Mulitza, S., Müller, P.J., Wefer, G., Zahn, R. (1999) Warming of the tropical Atlantic Ocean and slowdown of thermohaline circulation during the last deglaciation. *Nature*, **402**, 511-514.

Sagredo, E.A., Rupper, S., Lowell, T.V. (2014) Sensitivities of the equilibrium line altitude to temperature and precipitation changes along the Andes. *Quaternary Research*, **81**, 355-366.

Schildgen, T.F., Robinson, R.A.J., Savi, S., Phillips, W.M., Spencer, J.Q.G., Bookhagen, B., Scherler, D., Tofelde, S., Alonso, R.N., Kubik, P.W., Binnie, S.A., Strecker, M.R. (2016) Landscape response to late Pleistocene climate change in NW Argentina: Sediment flux modulated by basin geometry and connectivity. *Journal of Geophysical Research: Earth Surface*, **121**, 392-414.

Schmitt, J., Schneider, R., Elsig, J., Leuenberger, D., Lourantou, A., Chappellaz, J., Köhler, P., Joos, F., Stocker, T.F., Leuenberger, M., Fischer, H. (2012) Carbon isotope constraints on the deglacial $CO_2$ rise from ice cores. *Science*, **336**, 711-714.

Shakun, J.D., Clark, P.U., He, F., Marcott, S.A., Mix, A.C., Liu, Z., Otto-Bliesner, B., Schmittner, A., Bard, E. (2012) Global warming preceded by increasing carbon dioxide concentrations during the last deglaciation. *Nature*, **484**, 49-54.

Shakun, J.D., Clark, P.U., Marcott, S.A., Brook, E.J., Lifton, N.A., Caffee, M., Shakun, W.R. (2015) Cosmogenic dating of Late Pleistocene glaciation, southern tropical Andes, Peru. *Journal of Quaternary Science*, **30**, 841-847.

Smith, C.A., Lowell, T.V., Owen, L.A., Caffee, M.W. (2011) Late Quaternary glacial chronology on Nevado Illimani, Bolivia, and the implications for paleoclimatic reconstructions across the Andes. *Quaternary Research*, **75**, 1-10.

Smith, J.A., Finkel, R.C., Farber, D.L., Rodbell, D.T., Seltzer, G.O. (2005b) Moraine preservation and boulder erosion in the tropical Andes: interpreting old surface exposure ages in glaciated valleys. *Journal of Quaternary Science*, **20**, 735-758.

Smith, J.A., Rodbell, D.T. (2010) Cross-cutting moraines reveal evidence for North Atlantic influence on glaciers in the tropical Andes. *Journal of Quaternary Science*, **25**, 243-248.

Smith, J.A., Seltzer, G.O., Farber, D.L., Rodbell, D.T., Finkel, R.C. (2005a) Early Local Last Glacial Maximum in the Tropical Andes. *Science*, **308**, 678-681.

Stansell, N.D., Licciardi, J.M., Rodbell, D.T., Mark, B.G. (2017) Tropical ocean-atmospheric forcing of Late Glacial and Holocene glacier fluctuations in the Cordillera Blanca, Peru. *Geophysical Research Letters*, **44**, 4176-4185.

Stansell, N.D., Rodbell, D.T., Licciardi, J.M., Sedlak, C.M., Schweinsberg, A.D., Huss, E.G., Delgado, G.M., Zimmerman, S.H., Finkel, R.C. (2015) Late Glacial and Holocene glacier fluctuations at Nevado Huagurucho in the Eastern Cordillera of the Peruvian Andes. *Geology*, **43**, 747-750.

Steffen, D., Schlunegger, F., Preusser, F. (2009) Drainage basin response to climate change in the Pisco valley, Peru. *Geology*, **37**, 491-494.

Steffen, D., Schlunegger, F., Preusser, F. (2010) Late Pleistocene fans and terraces in the Majes valley, southern Peru, and their relation to climatic variations. *International Journal of Earth Sciences*, **99**, 1975-1989.

Stone, J.O. (2000) Air pressure and cosmogenic isotope production. *Journal of Geophysical Research*, **105**, 23753-23759.

Strecker, M.R., Alonso, R.N., Bookhagen, B., Carrapa, B., Hilley, G.E., Sobel, E.R., Trauth, M.H. (2007) Tectonics and climate of the southern Central Andes. *Annual Review of Earth and Planetary Sciences*, **35**, 747-787.

Strecker, M.R., Cerveny, P., Bloom, A.L., Malizia, D. (1989) Late Cenozoic tectonism and landscape development in the foreland of the Andes: Northern Sierras Pampeanas (26°-28°S), Argentina. *Tectonics*, **8**, 517-534.

Sylvestre F, Servant M, Servant-Vildary S, Causse C, Fournier M, Ybert J-P (1999) Lake-level chronology on the Southern Bolivian Altiplano (18◦–23◦S) during late-glacial time and the Early Holocene. *Quaternary Research,* **51**, 54–66.

Tapia, A. (1925) Apuntes sobre el glaciarismo pleistocenico del Nevado del Aconquija. *Anales Soc. Argentina de Estudios Geográficos*, **4**, 313-365.

Tchilinguirian, P., Pereyra, F.X. (2001) Geomorfología del sector Salinas Grandes-Quebrada de Humahuaca, provincia de Jujuy. *Revista de la Asociación Geológica Argentina*, **56**, 3-15.

Terrizzano, T.M., García Morabito, E., Christl, M., Likerman, J., Tobal, J., Yamin, M., Zech, R. (2017) Climatic and tectonic forcing on alluvial fans in the southern Central Andes. *Quaternary Science Reviews*, **172**, 131-141.

Thomas, E.R., Wolff, E.W., Mulvaney, R., Steffensen, J.P., Johnson, S.J., Arrowsmith, C., White, J.W.C., Vaughn, B., Popp, T. (2007) The 8.2 ka event from Greenland ice cores. *Quaternary Science Reviews*, **26**, 70-81.

Thompson, L.G., Davis, M.E., Mosley-Thompson, E., Sowers, T.A., Henderson, K.A., Zagarodnov, V.S., Lin, P.-N., Mikhalenko, V.N., Campen, R.K., Bolzan, J.F., Cole-Dai, J., Francou, B. (1998) A 25,000-Year Tropical Climate History from Bolivian Ice Core. *Science*, **282**, 1858-1864.

Thompson, L.G., Mosley-Thompson, E., Davis, M.E., Lin, P.-N., Henderson, K.A., Cole-Dai, J., Bolzan, J.F., Liu, K.-b. (1995) Late glacial stage and Holocene tropical ice core records from Huascarán, Peru. *Science*, **269**, 46-50.

Tiner, R.J., Negrini, R.M., Antinao, J.L., McDonald, E., Maldonado, A. (2018) Geophysical and geochemical constraints on the age and paleoclimate implications of Holocene lacustrine cores from the Andes of central Chile. *Journal of Quaternary Science*, **33**, 150-165.

Tofelde, S., Schildgen, T.F., Savi, S., Pingel, H., Wickert, A.D., Bookhagen, B., Wittmann, H., Alonso, R.N., Cottle, J., Strecker, M.R. (2017) 100 kyr fluvial cut-and-fill terrace cycles since the Middle Pleistocene in the southern Central Andes, NW Argentina. *Earth and Planetary Science Letters*, **473**, 141-153.

Torres, G.R., Lupo, L.C., Kulemeyer, J.J., Pérez, C.F. (2016) Palynological evidence of the geoecological belts dynamics from Eastern Cordillera of NW Argentina (23° S) during the Pre-Last Glacial Maximum. *Andean Geology*, **43**, 151-165.

Trauth, M.H., Alonso, R.A., Haselton, K.R., Hermanns, R.L., Strecker, M.R. (2000) Climate change and mass movements in the northwest Argentine Andes. *Earth and Planetary Science Letters*, **179**, 243–56.

Trauth, M.H., Bookhagen, B., Marwan, N., Strecker, M.R. (2003) Multiple landslide clusters record Quaternary climate changes in the NW Argentine Andes. *Palaeogeography, Palaeoclimatology, Palaeoecology*, **194**, 109-121.

Valet, J.-P., Meynadier, L., Guyodo, Y. (2005) Geomagnetic dipole strength and reversal rate over the past two million years. *Nature*, **435**, 802-805.

Vera, C., et al. (2006) Toward a unified view of the American monsoon systems. *Journal of Climate*, **19** (20), 4977–5000.

von Blanckenburg, F., Hewawasam, T., Kubik, P.W. (2004) Cosmogenic nuclide evidence for low weathering and denudation in the wet, tropical highlands of Sri Lanka. *Journal of Geophysical Research*, **109**, F03008.

WAIS Divide Project Members (2013) Onset of deglacial warming in West Antarctica driven by local orbital forcing. *Nature*, **500**, 440-444.

Wang, X., Auler, A.S., Edwards, R.L., Cheng, H., Ito, E., Wang, Y., Kong, X., Solheid, M. (2007) Millennial-scale precipitation changes in southern Brazil over the past 90,000 years. *Geophysical Research Letters*, **34**, L23701.

Ward, D., Thornton, R., Cesta, J. (2017) Across the Arid Diagonal: Deglaciation of the Western Andean Cordillera in southwest Bolivia and northern Chile. *Geographical Research Letters*, **43**, 667-696.

Ward, D.J., Cesta, J.M., Galewsky, J., Sagredo, E. (2015) Late Pleistocene glaciations of the arid subtropical Andes and new results from the Chajnantor Plateau, northern Chile. *Quaternary Science Reviews*, **128**, 98-116.

Wittmann, H., Malusà, M.G., Resentini, A., Garzanti, E., Niedermann, S. (2016) The cosmogenic record of mountain erosion transmitted across a foreland basin: source-to-sink analysis of in situ $^{10}$Be, $^{26}$Al and $^{21}$Ne in sediment of the Po river catchment. *Earth and Planetary Science Letters*, **452**, 258–271.

Zech, J., Terrizzano, C., García-Morabito, E., Veit, H., Zech, R. (2017) Timing and extent of Late Pleistocene glaciation in the arid Central Andes of Argentina and Chile (22°-41°S). *Geographical Research Letters*, **43**, 697-718.

Zech, J., Zech, R., Kubik, P.W., Veit, H. (2009a) Glacier and climate reconstruction at Tres Lagunas, NW Argentina, based on $^{10}$Be surface exposure dating and lake sediment analysis. *Palaeogeography, Palaeoclimatology, Palaeoecology*, **284**, 180-190.

Zech, J., Zech, R., May, J.-H., Kubik, P.W., Veit, H. (2010) Lateglacial and early Holocene glaciation in the tropical Andes caused by La Niña-like conditions. *Palaeogeography, Palaeoclimatology, Palaeoecology*, **293**, 248-254.

Zech, R., Kull, C., Veit, H. (2006) Late Quaternary glacial history in the Encierro Valley, northern Chile (29°S), deduced from $^{10}$Be surface exposure dating. *Palaeogeography, Palaeoclimatology, Palaeoecology*, **234**, 277-286.

Zech, R., Kull, Ch., Kubik, P.W., Veit, H. (2007a) Exposure dating of Late Glacial and pre-LGM moraines in the Cordon de Doña Rosa, Northern/Central Chile (~31°S). *Climate of the Past*, **3**, 1-14.

Zech, R., Kull, Ch., Kubik, P.W., Veit, H. (2007b) LGM and Late Glacial glacier advances in the Cordillera Real and Cochabamba (Bolivia) deduced from $^{10}$Be surface exposure dating. *Climate of the Past*, **3**, 623-635.

Zech, R., May, J.-H., Kull, C., Ilgner, J., Kubik, P.W., Veit, H. (2008) Timing of the late Quaternary glaciation in the Andes from ~15 to 40°S. *Journal of Quaternary Science*, **23**, 635-647.

Zech, R., Smith, J., Kaplan, M.R. (2009b) Chronologies of the Last Glacial Maximum and its Termination in the Andes (~10-55°S) Based on Surface Exposure Dating. In: Vimeux, F., Sylvestre, F., Khodri, M. (Eds) Past Climate Variability in South America and Surrounding Regions: From the Last Glacial Maximum to the Holocene*. Developments in Paleoenvironmental Research*, **14**, Springer, 61-88.

Zhang, Y., Chiessi, C.M., Mulitza, S., Sawakuchi, A.O., Häggi, C., Zabel, M., Portilho-Ramos, R.C., Schefuβ, E., Crivellari, S., Wefer, G. (2017) Different precipitation patterns across tropical South America during Heinrich and Dansgaard-Oeschger stadials. *Quaternary Science Reviews*, **177**, 1-9.

Zhang, Y., Chiessi, C.M., Multiza, S., Zabel, M., Trindade, R.I.F., Hollanda, M.H.B.M., Dantas, E.L., Govin, A., Tiedemann, R., Wefer, G. (2015) Origin of increased terrigenous supply to the NE South American continental margin during Heinrich Stadial 1 and the Younger Dryas. *Earth and Planetary Science Letters*, **432**, 493-500.

Zhang, Y., Zhang, X., Chiessi, C.M., Mulitza, S., Zhang, X., Lohmann, G., Prange, M., Behling, H., Zabel, M., Govin, A., Sawakuchi, A.O., Cruz, F.W., Wefer, G. (2016) Equatorial Pacific forcing of western Amazonian precipitation during Heinrich Stadial 1. *Scientific Reports*, **6**, 35866.

Zhou, J., Lau, K.-M. (1998) Does a Monsoon Climate Exist over South America? *Journal of Climate*, **11**, 1020-1040.